# Accepted Manuscript

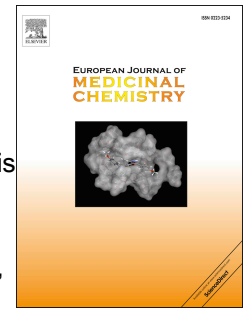


Antiproliferative hydrogen sulfide releasing evodiamine derivatives and their apoptosis inducing properties

Xu Hu, Runwei Jiao, Haonan Li, Xianhua Wang, Haoda Lyu, Xiang Gao, Fanxing Xu, Zhanlin Li, Huiming Hua, Dahong Li

PII: S0223-5234(18)30336-2

DOI: 10.1016/j.ejmech.2018.04.009

Reference: EJMECH 10358

To appear in: *European Journal of Medicinal Chemistry*

Received Date: 17 March 2018

Revised Date: 2 April 2018

Accepted Date: 3 April 2018

Please cite this article as: X. Hu, R. Jiao, H. Li, X. Wang, H. Lyu, X. Gao, F. Xu, Z. Li, H. Hua, D. Li, Antiproliferative hydrogen sulfide releasing evodiamine derivatives and their apoptosis inducing properties, *European Journal of Medicinal Chemistry* (2018), doi: 10.1016/j.ejmech.2018.04.009.

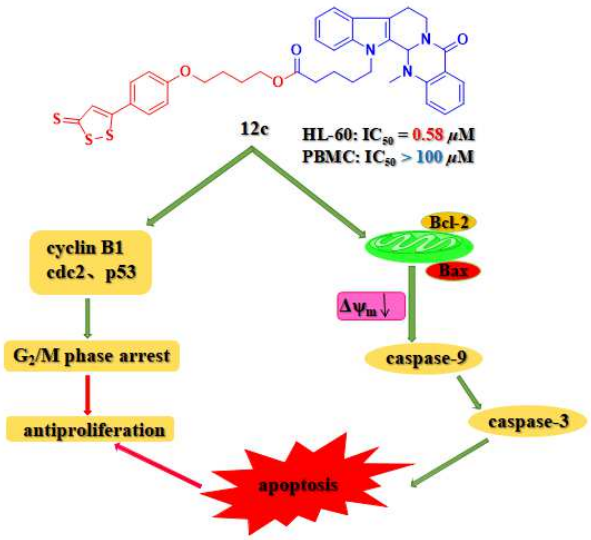

# Antiproliferative Hydrogen Sulfide Releasing Evodiamine Derivatives and Their Apoptosis Inducing Properties

Xu Hu[a], Runwei Jiao[a], Haonan Li[a], Xianhua Wang[b], Haoda Lyu[a], Xiang Gao[a], Fanxing Xu[c], Zhanlin Li[a], Huiming Hua[a], Dahong Li[a,*]

[a]*Key Laboratory of Structure-Based Drug Design & Discovery, Ministry of Education, and School of Traditional Chinese Materia Medica, Shenyang Pharmaceutical University, 103 Wenhua Road, Shenyang 110016, PR China*

[b]*School of Public Health, Qingdao University, 38 Dengzhou Road, Qingdao 266021, PR China*

[c]*Wuya College of Innovation, Shenyang Pharmaceutical University, 103 Wenhua Road, Shenyang 110016, PR China*



[*]Corresponding authors. E-mail addresses: lidahong0203@163.com (D. Li).

## ABSTRACT

To explore antitumor agents with high efficiency and selectivity, two series of 16 $H_2S$ donating evodiamine derivatives **8-12** were synthesized and characterized by $^1H$ NMR, $^{13}C$ NMR and HRMS. Their antiproliferative activities were tested against five cancer cell lines (Bel-7402, MCF-7, SGC-7901, Caco-2 and HL-60) and human normal peripheral blood mononuclear cells. Among them, compound **12c** showed the most potent inhibitory activities against human leukemia HL-60 and epithelial colorectal adenocarcinoma Caco-2 cells with $IC_{50}$ values of 0.58 and 2.02 $\mu$M, respectively. Additionally, high selectivity was also observed between human normal peripheral blood mononuclear cells and human leukemia HL-60 cells. Further mechanism studies confirmed that **12c** could induce apoptosis, arrest cell cycle at the $G_2$/M phase and lead to mitochondrial dysfunction in HL-60 cells. Furthermore, western blot assay demonstrated that **12c** induced the intrinsic apoptotic mitochondrial pathway by upregulating protein expression of Bax, cytochrome *c*, caspase-3, -9 and p53, and downregulating the relative levels of Bcl-2. The levels of cell cycle related proteins cyclin B1 and cdc2 were also downregulated in which $G_2$/M phase arrest was confirmed. Overall, **12c** possessed immense potential for the discovery of antitumor candidates with high efficiency and selectivity.


**Keywords:** natural product, antiproliferative activity, selectivity, apoptosis

## 1. Introduction

Evodiamine (**1**), which is a quinazolinocarboline alkaloid, was first isolated from the fruits of *Euodia rutaecarpa* Bentham [1]. It exhibits diverse pharmacological activities, such as anti-Alzheimer's disease [2,3], anti-cancer [4], analgesic activities [5], anti-obesity [6], anti-hyperlipidemia [7] and anti-inflammation [8]. It also plays a vital role for preventing osteolytic diseases [9], reducing caffeine-induced sleep disturbances and excitation [10], ameliorating liver fibrosis via TGF-$\beta$1/Smad signaling pathway [11,12], and inhibiting angiotensin □-induced cardiomyocyte hypertrophy [13]. Among them, the potential for evodiamine and its analogues as potent cancer chemotherapeutic agents has intrigued considerable research for new analogues with broad-spectrum antitumor activity [14–17], including human hepatoma [18], urothelial cell carcinoma [19], renal carcinoma [20], lung cancer [21], nasopharyngeal carcinoma [22], leukemia [23], gastric cancer [24], oral cancer [25], colorectal cancer [26], pancreatic cancer [27], bladder cancer [28], breast cancer [29], and ovarian cancer [30]. Moreover, the mechanisms which have been investigated demonstrated that evodiamine could induce cell growth arrest and apoptosis in human urothelial cell carcinoma and renal carcinoma cells [19,20]. Treatment of hepatocellular carcinoma cells with evodiamine exerted antiproliferative activity by inducing Akt-mediated apoptosis and a WW (two conserved tryptophans) domain-containing oxidoreductase-dependent pathway [18,31]. Besides, western blot analysis indicated that evodiamine could mediate the up-regulation of apoptotic proteins Bax/Bcl-2 and cleaved-caspase 3 in hepatocellular carcinoma cells [18]. Whereafter, some researchers reported the effect of evodiamine on the interaction between DNA methyltransferases (DNMTs) and target microRNAs during malignant

transformation of the colon by transforming growth factor-$\beta$1 (TGF-$\beta$1) [32]. Evodiamine showed broad antitumor activities through various mechanisms. However, moderate efficacy, as well as the poor selectivity between cancerous and normal cells, greatly impeded its further preclinical development and clinical applications. In order to overcome these disadvantages, novel evodiamine derivatives should be explored.

Hydrogen sulfide ($H_2S$) [33], a colorless and water-soluble gas with the smell of rotten eggs, is now recognized as an important gasotransmitter, after the extensive study of nitric oxide (NO) and carbon monoxide (CO). $H_2S$ is produced endogenously via enzymatic reactions of cysteine, homocysteine and cystathionine mediated by cystathionine-$\beta$-synthase (CBS), cystathionine-$\gamma$-lyase (CSE) and 3-mercaptopyruvate sulfurtransferase (3-MST) [34]. Over the past decade, numerous studies have shown that $H_2S$ plays significant roles in physiology and pathology regarding myocardial reperfusion injury [35], hypertension [36], atherosclerosis [37], stroke [38], neuroinflammation [39], diabetes mellitus [40] and so on. Recently, $H_2S$ was found to show anticancer activity [41,42], which could trigger apoptosis via activation of MAPK and caspase-3, and sulfhydration of NF-$\kappa$B [43], enhance cell proliferation of human gastric cancer AGS cells [44], promote autophagy of hepatocellular carcinoma cells through EGFR/ERK/MMP-2 and PI3K/Akt/mTOR signaling pathways [45,46], and induce C6 glioma cell growth through activation of the p38 MAPK/ERK1/2-COX-2 pathways [47]. However, $H_2S$ is not used directly in clinic because of uncontrollable dose and high toxicity. Researchers often use $H_2S$ releasing agents ($H_2S$ donors) to modulate $H_2S$ levels and enable new investigations [48,49]. It was reported the slow-releasing $H_2S$ donor, GYY4137, exhibited potent anti-hepatocellular carcinoma activity through blocking the signal transducer and STAT3 pathway [50,51]. Thereafter, $H_2S$-releasing diclofenac derivatives not only

increased the activity of anti-inflammatory and reduced the side effects of diclofenac, but also inhibited breast cancer-induced osteoclastogenesis and prevented osteolysis [52]. Thenceforward, increasing studies have been reported on the antitumor effects of $H_2S$ donors [53–57]. With the development of $H_2S$ donating derivatives (Fig. 1), many $H_2S$ donors were found, such as dithiothione derivatives ADTOH [58], *α*-thioctic acid [59], thiobenzamide derivatives [60], iminothioethers [61], cyclic acyl disulfides and acyl selenylsulfides [62], tetrasulfides [63] and 1,2,4-thiadiazolidin-3,5-diones [64]. In general, substantial progress has been achieved in the application of $H_2S$ donors towards the treatment of human cancers over the past decade. Therefore, design and synthesis of $H_2S$ releasing hybrids is an effective and promising strategy for cancer treatment.

In this study, we wanted to continue our studies [65,66] of evodiamine to seek highly selective antiproliferative drug candidates by combining the potent natural compound with $H_2S$ donors. Aforementioned predicament inspired us to synthesize 16 derivatives based on two kinds of exogenous $H_2S$ donors: ADTOH and *α*-thioctic acid. Resulting hybrids were evaluated against human cancer Bel-7402, MCF-7, SGC-7901, Caco-2 and HL-60 cell lines, and normal peripheral blood mononuclear cells (PBMCs) for antiproliferative activities. Additionally, further mechanisms regarding cell cycle progression, induction of apoptosis, dysfunction of mitochondrial membrane potential and expression of apoptosis-related and cell cycle-related proteins by representative derivative **12c** were also investigated.

## 2. Result and Discussion

### *2.1. Chemistry*

The synthetic routine of target compounds is illustrated in Scheme 1 and 2. First, **1**

was treated with corresponding bromohydrin (2-bromine ethanol, 3-bromine-1-propanol or 6-bromine-1-hexanol), bromate ethyl ester (ethyl bromoacetate, ethyl 4-bromobutyrate, ethyl 5-bromovalerate) in the presence of NaH and anhydrous *N*,*N*-dimethylformamide (DMF) to offer **2a–d** and **3a-c** in high yields. Then **3a-c** were hydrolyzed by potassium hydroxide to generate the intermediates **4a-c**. Next, the substitution reactions of **5** with corresponding dibromo reagents (dibromoethane, 1,3-dibromopropane, 1,4-dibromobutane) were completed smoothly under the condition of potassium carbonate and anhydrous acetone (Scheme 1).

Finally, the target $H_2S$ donating evodiamine derivatives **8a-d** were synthesized from **2a–d** accordingly with *α*-thioctic acid **7** in the presence of 4-dimethylaminopyridine/1-ethyl-3-(3-dimethylaminopropyl) carbodiimide hydrochloride (DMAP/EDCI) in anhydrous dichloromethane (DCM) at room temperature for 8-12h. The derivatives **9a-c** were got from **2a–d** by the reaction with **5** under the condition of DMAP/EDCI in anhydrous DCM. Then the $H_2S$ donor intermediates **6a-c** were treated with the evodiamine derivatives **4a-c** to give the target compounds **10a-c**, **11a-c** and **12a-c** in the presence of triethylamine (TEA) and anhydrous DMF (Scheme 2).

*2.2. Biological evaluation*

*2.2.1 Antiproliferative activity*

The antiproliferative activities of 16 target hybrids (**8a**–**d**, **9a-c**, **10a-c**, **11a-c** and **12a-c**) against five different kinds of human cancer cell lines (human hepatoma cell line Bel-7402, human breast carcinoma cell line MCF-7, human gastric carcinoma cell line SGC-7901, human epithelial colorectal adenocarcinoma cell line Caco-2 and human leukemic cell line HL-60) and PBMCs were tested, compared with lead compound evodiamine (**1**), ADTOH (**5**), *α*-thioctic acid (**7**) and positive control

5-fluorouracil (5-FU).

As shown in Table 1, most target compounds were sensitive to Caco-2 and HL-60 cell lines, which displayed more potent inhibitory activities than evodiamine, and some of them showed superior cytotoxic activities to 5-FU. While, in Bel-7402 and SGC-7901 cell lines, target compounds showed almost no cytotoxicity. In MCF-7 cell line, only **8a** was stronger than parent compound **1** with $IC_{50}$ value of 9.47 $\mu$M. Interestingly, **10a-c**, **11a-c**, **12a-c** incorporated with ADTOH showed stronger activities than **8a-d** with $\alpha$-thioctic acid against HL-60 cells. When R was $(CH_2)_2$ (**8a**), the antiproliferative activities were stronger than those with $(CH_2)_3$, $(CH_2)_3$-O-$(CH_2)_3$ and $(CH_2)_6$ (**8b-c**) against MCF-7 and HL-60 cells. For **12a–c**, the linkage of 4 carbons (**12c**) was more beneficial to antiproliferative activity than 2 carbons (**12a**) and 3 carbons (**12b**) against HL-60 cells. Comparing the antiproliferative activities of $H_2S$ releasing evodiamine derivatives (**8a**, **10b**, **11b-c** and **12a-c**) with those of $H_2S$ donors (**5** and **7**) and evodiamine, it could be found that the hybrids showed better antiproliferative properties. Furthermore, in order to investigate whether the hybrids exhibited selective antiproliferative activities between normal cells and malignant cancer cells, all hybrids were screened against PBMCs with evodiamine as control. All the target compounds exhibited inconsequential antiproliferative activity ($IC_{50}$ > 100 $\mu$M) in comparison with evodiamine ($IC_{50}$ 20.96 $\mu$M). Among these hybrids, **12c** exhibited the most potent activities against HL-60 cells with $IC_{50}$ value of 0.58 $\mu$M and good selectivity between tumor and normal cells. So, **12c** was selected for further mechanism study to search for a potentially safer chemotherapy agent.

### *2.2.2 Cell cycle analysis*

The effects of **12c** on HL-60 cell cycle were first examined. HL-60 cells were

treated with different concentrations of **12c** (0, 0.3, 0.6 and 1.2 $\mu$M) for 48 h and stained with propidium iodide (PI), followed by flow cytometry analysis. Non-treated cells were used as control. As shown in Fig. 2, the cells in $G_1$, S and $G_2$/M phases of control group accounted for 65.75%, 24.06% and 10.19%, respectively. After treatment with different concentrations of **12c** for 48 h, the cells of $G_2$/M phase increased from 10.19% to 11.41%, 16.63% and 22.02%, respectively. The results indicated that **12c** suppressed HL-60 cell proliferation through inducing cell cycle arrest at $G_2$/M phase.

*2.2.3 The morphological analysis by Hoechst 33258 staining*

The remarkable changes of morphological features, such as cell shrinkage, chromatin condensation, the rupture of cell membrane and the nuclear fragmentation are the characteristics of apoptotic cells [67]. Hoechst 33258, which stains the cell nuclei and emits fluorescence allowing the visualization of nuclear morphological changes, is a membrane permeable dye. Thus, Hoechst 33258 staining were carried out under fluorescent microscope on **12c** (0, 0.3, 0.6 and 1.2 $\mu$M) treated HL-60 cells to determine whether apoptosis was triggered during inhibition of cell growth. As shown in Fig. 3, control cells were consistently stained with Hoechst 33258 and presented round homogeneous nuclei, without morphological changes, while the **12c** treated HL-60 cells exhibited bright chromatin condensation and nuclear fragmentation, a sign of apoptosis. The stain results certified apoptosis was involved in **12c** treated HL-60 cells.

*2.2.4 Cell apoptosis assay*

Apoptosis is a natural process of programmed cell death. However, tumor cells can divide relentlessly without programmed cell death, which mainly due to the lack of apoptosis. Thus, chemical induced apoptosis in tumor cells is pivotal to cancer

therapy [68]. Therefore, to further certify **12c** induced apoptosis in HL-60 cells, an annexin V-FITC/PI binding assay was performed. HL-60 cells were treated with **12c** at indicated concentrations (0, 0.3, 0.6 and 1.2 $\mu$M), then the percentages of apoptotic cells were measured by flow cytometry. As shown in Fig. 4, 48 h after the treatment of **12c** gave substantial rise to the apoptotic ratios from 3.42% of vehicle control to 11.27% (0.3 $\mu$M), 35.06% (0.8 $\mu$M) and 60.68% (1.2 $\mu$M) for different concentrations applied in a concentration-dependent manner. Aforementioned results demonstrated that **12c** exerted its antiproliferative effects possibly by inducing apoptosis in HL-60 cells.

*2.2.5 Mitochondria membrane potential analysis*

The mitochondrion is an organelle that plays an essential role in the induction and control of apoptosis. Its dysfunction, including the loss of mitochondrial membrane potential, is a key event that takes place during drug-induced apoptosis. Both the inner and the outer mitochondrial membranes were involved in these changes, which sequentially lead to dissipate inner transmembrane potential, promote mitochondrial permeability transition and induce the release of pro-apoptotic proteins [69]. $H_2S$ is also known to induce apoptosis by activating the intrinsic mitochondrion-mediated pathways [70]. In an effort to disclose the participation of mitochondria pathway in **12c** induced apoptosis of HL-60 cells, the changes of mitochondrial membrane potentials were assessed. HL-60 cells were treated with different concentrations of **12c** (0.3, 0.6 and 1.2 $\mu$M) and vehicle solvent for 48 h incubation, then staining with the lipophilic cationic fluorescent probe 5,5′,6,6′-tetrachloro-1,1′,3,3′-tetraethylbenzimidazol-carbocyanine iodide (JC-1). JC-1 is commercially available. In normal cells, JC-1 aggregates in the mitochondria and spontaneously forms complexes which fluoresce red. In apoptosis or necrotic cells,

JC-1 exists in the monomeric form and stains the cytosol green. After that, flow cytometry analysis was established to measure the cells with collapsed mitochondrial membrane. These results were summarized in Fig. 5, the percentage of apoptotic cells increased from 7.65% of control, to 13.33%, 21.32% and 35.01%, respectively. It was clear that hybrid **12c** could induce apoptosis in HL-60 cells through mitochondria related pathway.

*2.2.6 Effects on apoptosis-related proteins*

Abnormal proliferation of cancer cells are mainly due to damage of cell cycle regulation. So, disruption of cell cycle by therapeutic agents can lead to tumour growth arrest and ultimately to apoptosis, contributing to cancer therapy. Previously, some studies have confirmed cells with CDK1 (cyclin B1/cdc2 complex) inhibitor would tend to be arrested at the $G_2$/M phase while cells with CDK1 activator would be favoured to enter and then proceed through mitosis [71]. Furthermore, tumor suppressor gene p53 is critically involved in cell cycle regulation, DNA repair and programmed cell death. It can also regulate $G_2$/M transition through downregulating the intracellular level of cyclin B1 and cdc2 [72]. Recently, it has been demonstrated that endogenous $H_2S$ has a relationship with mitochondria-mediated apoptosis [73]. Mitochondria represent the central checkpoint in propagating apoptotic signalling pathways, upon exposure to apoptotic stimuli, it can activate apoptosis-related proteins such as Bax (proapoptotic protein) and Bcl-2 (antiapoptotic protein) to enter mitochondria, which induce the mitochondria to release cytochrome *c* and, in turn, activate the caspase-9 and -3, finally triggering the execution of apoptosis [74]. To explore the mediative mechanism of aforementioned apoptosis related proteins behind **12c** induced apoptosis in HL-60 cells, correspondent western blot analysis was performed, and subsequent results were summarized in Fig. 6. After 48 h treatment,

**12c** significantly upregulated the expression of p53, together with downregulation of cyclin B1 and cdc2. It could also upregulate proteins expression of proapoptotic Bax, caspase-3, -9 and cytochrome *c*, and suppress of antiapoptotic Bcl-2 protein expression. Thus, it was illuminated that **12c** induced cell apoptosis via the mitochondria-dependent pathway.

## 3. Conclusion

To summarize, two novel series of evodiamine derivatives capable of releasing $H_2S$ were designed and synthesized for anticancer therapeutics. The antiproliferative activities of all the target compounds were tested against human cancer Bel-7402, MCF-7, SGC-7901, Caco-2 and HL-60 cell lines, and human normal PBMCs. The most effective one, conjugate **12c** exhibited cytotoxicity against HL-60 and Caco-2 cell lines with $IC_{50}$ values of 0.58 and 2.02 $\mu$M, respectively. Amazingly, antiproliferative evaluation showed that efficacy enhancement accompanied with improved selectivity. Hence, **12c** was chosen for further investigation in order to reveal the cellular mechanisms in HL-60 cell lines. The results demonstrated that **12c** showed strong effects which could induce cell apoptosis and arrest cell cycle at the $G_2$/M stage. Moreover, incubation with **12c** increased the number of cells with collapsed mitochondrial membrane potentials at low concentrations, so the mitochondrial pathway would be involved in apoptosis. Subsequently, western blot analysis confirmed that **12c** induced apoptosis via mitochondrial related pathway, since **12c** increased the expression of Bax, cytochrome *c*, caspase-9, -3 and p53, and reduced the relative levels of Bcl-2, cyclin B1 and cdc2. In conclusion, **12c**, a potent compound with $H_2S$ releasing ability, offers a good strategy for the discovery of antitumor agents with high efficiency and selectivity.

## 4. Experimental

### *4.1. Chemistry*

Chemicals and solvents were purchased from commercial sources. Evodiamine was obtained from Zelang Biological Techology Co., Ltd. (Nanjing, China) with the purity > 95%. Further purification by standard methods were employed when necessary. $^{1}$H NMR and $^{13}$C NMR spectra were recorded on a Bruker ARX-400 NMR spectrometer in the indicated solvents (TMS as internal standard): the values of the chemical shifts were expressed in $\delta$ values (ppm) and the coupling constants (*J*) in Hz. Mass spectra were obtained on Agilent 1100 Ion trap mass spectrometer. High-resolution mass spectra (HR-MS) were carried out on Agilent Q-TOF B.05.01 (B5125.2).

#### *4.1.1. General procedures to synthesize **2a-d**, **4a-c** and **6a-c***

Compound **1** (91 mg, 0.3 mmol) was dissolved in 5 mL anhydrous DMF. Then NaH (10 mg, 0.36 mmol) was added to a solution of **1** and stirred at 0 □ for 0.5 h. The corresponding bromhydrin was added dropwise to reaction solution by stirring at room temperature for another 3 h, then the mixture was poured into 10 mL of $H_2O$ and extracted with DCM (10 mL × 3). The organic layer was combined, washed with water and saturated NaCl solution, sequentially, dried over anhydrous $Na_2SO_4$ and concentrated *in vacuo*. The crude products **2a-d** were purified by column chromatography (PE/EA 5:1~3:1 v/v).

Compound **1** (91 mg, 0.3 mmol) was dissolved in 5 mL anhydrous DMF. NaH (10 mg, 0.36 mmol) was added to a solution of **1** and stirred at 0 □ for 0.5 h**.** The corresponding bromate ethyl ester was added dropwise to reaction solution by stirring at 80 □ for another 12 h, then the mixture was poured into 10 mL of $H_2O$ and

extracted with DCM (10 mL × 3). The organic layer was combined, washed with water and saturated NaCl solution, sequentially, dried over anhydrous $Na_2SO_4$ and concentrated *in vacuo*. The crude products **3a-c** were purified by column chromatography (PE/EA 20:1~10:1 v/v) to give **3**. Next, compounds **3a-c** were hydrolysed in a solution of methanol/potassium hydroxide (MeOH/KOH) by stirring at room temperature for 2 h. After completion of the reaction as indicated by TLC, the mixture was concentrated, then $H_2O$ was added and the solution was carefully acidized with 0.6 M hydrochloric acid. The combined extracts were dried over filtration, and evaporated to yield **4a-c**.

Compound **5** (226 mg, 1 mmol), potassium carbonate (220 mg, 3 mmol) and corresponding dibromo alkyl reagents were dissolved in 5 mL anhydrous acetone and heated under reflux for 8 h. After that, the reaction mixture was cooled to room temperature, evaporated under reduced pressure, and the crude product was purified by flash chromatography eluting with petroleum ether/ethyl acetate (10:1) to afford **6a-c**.

*4.1.2. General procedures to synthesize **8a-d**, **9a-c**, **10a-c**, **11a-c** and **12a-c***

A solution of *α*-thioctic acid (0.1 mmol), EDCI (0.3 mmol) and compound **2a** (40 mg, 0.1 mmol) in anhydrous DCM (5 mL) with catalytic amount of DMAP was stirred mechanically at room temperature until esterification was complete. The mixture was poured into 10 mL of $H_2O$, and extracted with DCM (10 mL × 3). The organic layers were combined, washed with saturated NaCl solution, dried over anhydrous $Na_2SO_4$, and concentrated *in vacuo*. The residues were purified by chromatography on silica gel (petroleum ether-ethyl acetate 10:1) to afford **8a** (35 mg). The preparation and workup of compounds **8b-d** were similar to **8a**.

Compounds **9a-c** were prepared using a procedure similar to that of **8a** except

ADTOH were used instead of *α*-thioctic acid. Compounds **4a-c** were used instead of compound **2**. Chromatography on silica gel with (petroleum ether-ethyl acetate 8:1) as eluent gave the products.

A mixture of **4a** (18 mg, 0.05 mmol), **6a** (20 mg, 0.05 mmol), catalytic amount of TEA and anhydrous DMF (5 mL) was heated at 80 □ with stirring for 8 h. After that, the reaction mixture was cooled, diluted with $H_2O$ (10 mL) and extracted with ethyl acetate (10 mL × 3). The organic layers were combined, washed with saturated NaCl solution, dried over anhydrous $Na_2SO_4$ and concentrated *in vacuo*. The residues were purified by chromatography on silica gel (petroleum ether-ethyl acetate 6:1) to afford **10a** (15 mg). The preparation and workup of **10b-c**, **11a-c** and **12a-c** were similar to **10a**.

*4.1.2.1 Compound **8a***. Pale yellow solid, yield: 55%. $^1$H NMR ($CDCl_3$, 400 MHz), *δ* (ppm): 8.15 (dd, *J* = 7.8, 1.2 Hz, 1H, Ar-H), 7.61 (d, *J* = 7.8 Hz, 1H, Ar-H), 7.51 (td, *J* = 7.9, 1.2 Hz, 1H, Ar-H), 7.45 (d, *J* = 7.9 Hz, 1H, Ar-H), 7.31 (d, *J* = 7.2 Hz, 1H, Ar-H), 7.28 (m, 1H, Ar-H), 7.22 (m, 1H, Ar-H), 7.18 (d, *J* = 7.2 Hz, 1H, Ar-H), 6.02 (s, 1H, N-CH-N), 4.92 (m, 1H, N-$CH_2$), 4.74 (m, 1H, 13-N-$CH_2$), 4.42 (m, 2H, -COO$CH_2$), 3.46 (m, 1H, 13-N-$CH_2$), 3.21 (m, 1H, N-$CH_2$), 3.15 (m, 1H, -$CH_2$), 3.10 (m, 1H, -$CH_2$), 3.04 (m, 1H, -$CH_2$), 2.89 (m, 1H, -$CH_2$), 2.40 (s, 3H, N-$CH_3$), 2.17 (m, 2H, -$CH_2$), 1.85 (m, 1H, -S-CH-), 1.23–1.60 (m, 8H, -$CH_2$); $^{13}$C NMR ($CDCl_3$, 100 MHz), *δ* (ppm): 173.06, 164.57, 150.92, 137.70, 133.07, 129.08, 128.49, 125.93, 124.56, 124.26, 123.42, 123.03, 120.06, 119.18, 113.95, 109.83, 68.15, 62.95, 56.32, 42.54, 40.26, 39.34, 38.56, 36.62, 34.55, 33.94, 28.64, 24.47, 20.43; HRMS (ESI) *m/z* calcd for $C_{29}H_{33}N_3HO_3S_2$ $[M+H]^+$ 536.2036, found 536.2057.

*4.1.2.2 Compound **8b***. Pale yellow solid, yield: 66%. $^1$H NMR ($CDCl_3$, 600 MHz), *δ* (ppm): 8.14 (dd, *J* = 7.8, 1.4 Hz, 1H, Ar-H), 7.61 (d, *J* = 7.8 Hz, 1H, Ar-H), 7.51 (m,

1H, Ar-H), 7.38 (m, 1H, Ar-H), 7.30 (m, 1H, Ar-H), 7.25 (m, 1H, Ar-H), 7.21 (m, 1H, Ar-H), 7.18 (m, 1H, Ar-H), 5.98 (s, 1H, N-CH-N), 4.91 (m, 1H, N-$CH_2$), 4.54 (m, 1H, 13-N-$CH_2$), 4.28 (m, 1H, 13-N-$CH_2$), 4.17 (m, 1H, -$COOCH_2$), 4.03 (m, 1H, -$COOCH_2$), 3.54 (m, 1H, N-$CH_2$), 3.20 (m, 2H, -$CH_2$), 3.11 (m, 1H, -$CH_2$), 3.03 (m, 1H, -$CH_2$), 2.89 (m, 1H, -$CH_2$), 2.45 (m, 1H, -$CH_2$), 2.40 (s, 3H, N-$CH_3$), 2.18 (m, 2H, -$CH_2$), 2.12 (m, 2H, -$CH_2$), 1.89 (m, 1H, -S-CH-), 1.34–1.65 (m, 6H, -$CH_2$); $^{13}$C NMR ($CDCl_3$, 150 MHz) $\delta$ (ppm): 173.32, 164.62, 150.98, 137.17, 133.02, 129.07, 128.41, 125.93, 124.47, 124.26, 123.23, 122.88, 119.86, 119.24, 113.45, 109.61, 68.02, 61.61, 56.45, 40.70, 40.35, 39.37, 38.60, 36.48, 34.61, 33.92, 29.25, 28.82, 24.58, 20.42; HRMS (ESI) *m/z* calcd for $C_{30}H_{35}N_3HO_3S_2$ $[M+H]^+$ 550.2193, found 550.2176.

*4.1.2.3 Compound* ***8c***. Pale yellow solid, yield: 65%. $^1$H NMR ($CDCl_3$, 600 MHz), $\delta$ (ppm): 8.13 (dd, $J$ = 7.8, 1.4 Hz, 1H, Ar-H), 7.61 (d, $J$ = 7.8 Hz, 1H, Ar-H), 7.49 (m, 1H, Ar-H), 7.43 (m, 1H, Ar-H), 7.28 (m, 1H, Ar-H), 7.23 (m, 1H, Ar-H), 7.20 (m, 1H, Ar-H), 7.17 (m, 1H, Ar-H), 6.00 (s, 1H, N-CH-N), 4.90 (m, 1H, N-$CH_2$), 4.56 (m, 1H, 13-N-$CH_2$), 4.28 (m, 1H, 13-N-$CH_2$), 4.08 (m, 1H, -$COOCH_2$), 4.03 (m, 1H, -$COOCH_2$), 3.55 (m, 1H, N-$CH_2$), 3.42 (m, 1H, -$CH_2$-O-$CH_2$), 3.37 (m, 2H, -$CH_2$-O-$CH_2$), 3.34 (m, 1H, -$CH_2$-O-$CH_2$), 3.18 (m, 2H, -$CH_2$), 3.10 (m, 1H, -$CH_2$), 3.03 (m, 1H, -$CH_2$), 2.89 (m, 1H, -$CH_2$), 2.45 (m, 1H, -$CH_2$), 2.40 (s, 3H, N-$CH_3$), 2.30 (m, 2H, -$CH_2$), 2.06 (m, 2H, -$CH_2$), 1.89 (m, 1H, -S-CH-), 1.62–1.77 (m, 6H,-$CH_2$), 1.47 (m, 2H, -$CH_2$); $^{13}$C NMR ($CDCl_3$, 150 MHz) $\delta$ (ppm): 173.51, 164.69, 151.02, 137.35, 132.94, 128.98, 128.62, 125.79, 124.18, 124.13, 123.13, 122.68, 119.66, 119.05, 113.16, 109.90, 67.92, 67.65, 67.39, 61.51, 56.45, 40.68, 40.33, 39.41, 38.57, 36.39, 34.69, 34.13, 30.29, 29.06, 28.87, 24.78, 20.48; HRMS (ESI) *m/z* calcd for $C_{33}H_{41}N_3NaO_4S_2$ $[M+Na]^+$ 630.2431, found 630.2501.

*4.1.2.4 Compound* ***8d***. Pale yellow solid, yield: 59%. $^1$H NMR ($CDCl_3$, 400 MHz),

$\delta$ (ppm): 8.15 (dd, $J$ = 7.8, 1.2 Hz, 1H, Ar-H), 7.61 (d, $J$ = 7.8 Hz, 1H, Ar-H), 7.50 (m, 1H, Ar-H), 7.39 (m, 1H, Ar-H), 7.30 (m, 1H, Ar-H), 7.23 (m, 1H, Ar-H), 7.19 (m, 1H, Ar-H), 7.16 (m, 1H, Ar-H), 5.97 (s, 1H, N-CH-N), 4.91 (m, 1H, N-$CH_2$), 4.37 (m, 1H, 13-N-$CH_2$), 4.19 (m, 1H, 13-N-$CH_2$), 4.03 (m, 2H, -COO$CH_2$), 3.55 (m, 1H, -$CH_2$), 3.21 (m, 1H, N-$CH_2$), 3.15 (m, 1H, -$CH_2$), 3.10 (m, 1H, -$CH_2$), 3.03 (m, 1H, -$CH_2$), 2.89 (m, 1H, -$CH_2$), 2.45 (m, 1H, -$CH_2$), 2.40 (s, 3H, N-$CH_3$), 2.28 (m, 2H, -$CH_2$), 1.90 (m, 2H, -$CH_2$), 1.84 (s, 1H, -S-CH-), 1.38–1.73 (m, 12H, -$CH_2$); $^{13}$C NMR ($CDCl_3$, 100 MHz) $\delta$ (ppm): 173.53, 164.58, 150.95, 137.19, 132.96, 129.01, 128.33, 125.75, 124.24, 124.15, 123.08, 122.62, 119.57, 119.06, 113.10, 109.80, 68.12, 64.22, 56.38, 43.89, 40.26, 39.37, 38.51, 36.51, 34.62, 34.10, 30.13, 28.78, 28.59, 26.88, 25.80, 24.73, 20.42; HRMS (ESI) *m/z* calcd for $C_{33}H_{41}N_3HO_3S_2$ $[M+H]^+$ 592.2662, found 592.2677.

*4.1.2.5 Compound* ***9a***. Brownish red solid, yield: 70%. $^1$H NMR ($CDCl_3$, 400 MHz) $\delta$ (ppm): 8.15 (d, $J$ = 7.8 Hz, 1H, Ar-H), 7.66 (m, 3H, Ar-H), 7.52 (m, 2H, Ar-H), 7.36 (m, 3H, Ar-H), 7.30 (m, 1H, Ar-H), 7.25 (m, 1H, Ar-H), 7.23 (s, 1H, 4*H*-1,2-dithiole-3-thione), 7.17 (d, $J$ = 7.8 Hz, 1H, Ar-H), 6.00 (s, 1H, N-CH-N), 5.44 (m, 1H, 13-N-$CH_2$), 5.25 (m, 1H, 13-N-$CH_2$), 4.94 (m, 1H, N-$CH_2$), 3.26 (m, 1H, N-$CH_2$), 3.06 (m, 1H, -$CH_2$), 2.94 (m, 1H, -$CH_2$), 2.44 (s, 3H, N-$CH_3$); $^{13}$C NMR ($CDCl_3$, 100 MHz) $\delta$ (ppm): 215.64, 171.23, 166.77, 164.59, 153.13, 151.22, 137.94, 136.32, 133.20, 131.04, 129.83, 129.29, 128.99, 128.44 (×2), 126.29, 125.10, 123.69, 123.61, 122.55 (×2), 120.80, 119.57, 114.74, 109.08, 68.33, 65.71, 45.54, 39.42, 20.35; MS (ESI) *m/z* calcd for $C_{30}H_{23}N_3HO_3S_3$ $[M+H]^+$ 569.1, found 569.8.

*4.1.2.6 Compound* ***9b***. Brownish red solid, yield: 30%. $^1$H NMR ($CDCl_3$, 400 MHz) $\delta$ (ppm): 8.14 (dd, $J$ = 7.8, 1.2 Hz, 1H, Ar-H), 7.72 (m, 1H, Ar-H), 7.61 (d, $J$ = 8.5 Hz, 2H, Ar-H), 7.53 (m, 1H, Ar-H), 7.50 (m, 1H, Ar-H), 7.46 (m, 1H, Ar-H), 7.38

(s, 1H, 4*H*-1,2-dithiole-3-thione), 7.31 (m, 1H, Ar-H), 7.21 (m, 2H, Ar-H), 7.06 (d, *J* = 8.5 Hz, 2H, Ar-H), 6.01 (s, 1H, N-CH-N), 4.92 (m, 1H, N-$CH_2$), 4.57 (m, 1H, 13-N-$CH_2$), 4.36 (m, 1H, 13-N-$CH_2$), 3.20 (m, 1H, N-$CH_2$), 3.04 (m, 1H, -$CH_2$), 2.91 (m, 1H, -$CH_2$), 2.65 (m, 2H, -$CH_2$), 2.41 (s, 3H, N-$CH_3$), 2.30 (m, 2H, -$CH_2$); $^{13}$C NMR ($CDCl_3$, 100 MHz) $\delta$ (ppm): 215.64, 171.61, 170.79, 164.67, 153.38, 150.95, 137.41, 136.18, 133.10, 131.04, 129.41, 129.17, 128.97, 128.32 (×2), 125.96, 124.50, 123.30, 123.11, 122.82 (×2), 120.02, 119.31, 113.85, 109.82, 68.21, 65.70, 50.97, 42.90, 31.60, 25.14, 20.49; HRMS (ESI) *m/z* calcd for $C_{32}H_{27}N_3NaO_3S_3$ $[M+Na]^+$ 620.1040, found 620.1107.

*4.1.2.7 Compound* ***9c***. Brownish red solid, yield: 46%. $^1$H NMR ($CDCl_3$, 400 MHz) $\delta$ (ppm): 8.14 (dd, *J* = 7.8, 1.2 Hz, 1H, Ar-H), 7.64 (d, *J* = 8.7 Hz, 2H, Ar-H), 7.61 (m, 1H, Ar-H), 7.49 (m, 1H, Ar-H), 7.40 (m, 1H, Ar-H), 7.38 (s, 1H, 4*H*-1,2-dithiole-3-thione), 7.29 (m, 1H, Ar-H), 7.17–7.24 (m, 3H, Ar-H), 7.13 (d, *J* = 8.7 Hz, 2H, Ar-H), 5.99 (s, 1H, N-CH-N), 4.91 (m, 1H, N-$CH_2$), 4.45 (m, 1H, 13-N-$CH_2$), 4.28 (m, 1H, 13-N-$CH_2$), 3.20 (m, 1H, N-$CH_2$), 3.03 (m, 1H, -$CH_2$), 2.90 (m, 1H, -$CH_2$), 2.62 (m, 2H, -$CH_2$), 2.41 (s, 3H, N-$CH_3$), 1.98 (m, 2H, -$CH_2$), 1.82 (m, 2H, -$CH_2$); $^{13}$C NMR ($CDCl_3$, 100 MHz) $\delta$ (ppm): 215.60, 171.64, 171.07, 164.65, 153.53, 150.99, 137.25, 136.15, 133.08, 129.35, 129.12, 128.37, 128.32 (×2), 125.92, 124.46, 124.25, 123.25, 122.89 (×3), 119.84, 119.27, 113.49, 109.78, 68.24, 43.63, 39.43, 36.63, 33.94, 29.64, 22.46, 20.48; HRMS (ESI) *m/z* calcd for $C_{33}H_{29}N_3NaO_3S_3$ $[M+Na]^+$ 634.1263, found 634.1219.

*4.1.2.8 Compound* ***10a***. Brownish red solid, yield: 50%. $^1$H NMR ($CDCl_3$, 400 MHz) $\delta$ (ppm): 8.12 (d, *J* = 7.8 Hz, 1H, Ar-H), 7.71 (m, 1H, Ar-H), 7.61 (m, 1H, Ar-H), 7.58 (d, *J* = 8.8 Hz, 2H, Ar-H), 7.52 (m, 1H, Ar-H), 7.44 (m, 1H, Ar-H), 7.39 (s, 1H, 4*H*-1,2-dithiole-3-thione), 7.24 (m, 1H, Ar-H), 7.19 (m, 1H, Ar-H), 7.13 (d, *J*

= 7.8 Hz, 1H, Ar-H), 6.86 (d, *J* = 8.8 Hz, 2H, Ar-H), 5.93 (s, 1H, N-CH-N), 5.28 (m, 1H, 13-N-$CH_2$), 5.02 (m, 1H, 13-N-$CH_2$), 4.90 (m, 1H, N-$CH_2$), 4.57 (m, 1H, O-$CH_2$-$CH_2$-O), 4.49 (m, 1H, O-$CH_2$-$CH_2$-O), 4.18 (m, 2H, O-$CH_2$-$CH_2$-O), 3.17 (m, 1H, N-$CH_2$), 3.00 (m, 1H, -$CH_2$), 2.90 (m, 1H, -$CH_2$), 2.39 (s, 3H, N-$CH_3$); $^{13}$C NMR ($CDCl_3$, 100 MHz) $\delta$ (ppm): 215.34, 172.67, 168.69, 164.50, 161.49, 150.92, 137.88, 135.01, 133.02, 131.03, 129.14, 128.96, 128.79 (×2), 126.16, 124.95, 124.81, 123.55, 123.37, 120.50, 119.37, 115.51 (×2), 114.31, 109.15, 68.17, 66.07, 65.68, 63.44, 45.30, 30.70, 20.33; HRMS (ESI) *m/z* calcd for $C_{32}H_{27}N_3NaO_4S_3$ $[M+Na]^+$ 636.1056, found 636.1002.

*4.1.2.9 Compound* ***10b***. Brownish red solid, yield: 20%. $^1$H NMR ($CDCl_3$, 600 MHz) $\delta$ (ppm): 8.14 (d, *J* = 7.8 Hz, 1H, Ar-H), 7.60 (m, 1H, Ar-H), 7.58 (d, *J* = 8.6 Hz, 2H, Ar-H), 7.48 (m, 1H, Ar-H), 7.43 (m, 1H, Ar-H), 7.37 (s, 1H, 4*H*-1,2-dithiole-3-thione), 7.28 (m, 1H, Ar-H), 7.23 (m, 1H, Ar-H), 7.19 (m, 1H, Ar-H), 7.17 (m, 1H, Ar-H), 6.93 (d, *J* = 8.6 Hz, 2H, Ar-H), 5.94 (s, 1H, N-CH-N), 4.90 (m, 1H, N-$CH_2$), 4.43 (m, 2H, O-$CH_2$-$CH_2$-O), 4.26 (m, 2H, O-$CH_2$-$CH_2$-O), 4.12 (m, 2H, 13-N-$CH_2$), 3.18 (m, 1H, N-$CH_2$), 3.01 (m, 1H, -$CH_2$), 2.88 (m, 1H, -$CH_2$), 2.42 (m, 2H, -$CH_2$), 2.38 (s, 3H, N-$CH_3$), 2.18 (m, 2H, -$CH_2$); $^{13}$C NMR ($CDCl_3$, 150 MHz) $\delta$ (ppm): 215.29, 172.79, 172.60, 164.63, 161.70, 150.96, 137.34, 134.94, 133.04, 129.10, 128.75 (×2), 128.34, 128.24, 125.86, 124.80, 124.48, 123.31, 122.94, 119.88, 119.20, 115.58 (×2), 113.58, 109.85, 68.12, 66.15, 62.64, 53.57, 43.02, 39.38, 31.46, 25.30, 20.47; HRMS (ESI) *m/z* calcd for $C_{34}H_{31}N_3NaO_4S_3$ $[M+Na]^+$ 664.1369, found 664.1323.

*4.1.2.10 Compound* ***10c***. Brownish red solid, yield: 20%. $^1$H NMR ($CDCl_3$, 600 MHz) $\delta$ (ppm): 8.14 (d, *J* = 7.8 Hz, 1H, Ar-H), 7.60 (d, *J* = 7.8 Hz, 1H, Ar-H), 7.56 (d, *J* = 8.6 Hz, 2H, Ar-H), 7.49 (m, 1H, Ar-H), 7.37 (m, 1H, Ar-H), 7.36 (s, 1H,

4*H*-1,2-dithiole-3-thione), 7.28 (m, 1H, Ar-H), 7.24 (m, 1H, Ar-H), 7.21 (m, 1H, Ar-H), 7.17 (m, 1H, Ar-H), 6.91 (d, *J* = 8.6 Hz, 2H, Ar-H), 5.95 (s, 1H, N-CH-N), 4.90 (m, 1H, N-$CH_2$), 4.41 (m, 2H, O-$CH_2$-$CH_2$-O), 4.37 (m, 1H, 13-N-$CH_2$), 4.21 (m, 1H, 13-N-$CH_2$), 4.17 (m, 2H, O-$CH_2$-$CH_2$-O), 3.16 (m, 1H, N-$CH_2$), 3.01 (m, 1H, -$CH_2$), 2.88 (m, 1H, -$CH_2$), 2.40 (m, 2H, -$CH_2$), 2.38 (s, 3H, N-$CH_3$), 1.87 (m, 2H, -$CH_2$), 1.73 (m, 2H, -$CH_2$); $^{13}$C NMR ($CDCl_3$, 150 MHz) $\delta$ (ppm): 215.29, 173.07, 172.08, 164.66, 161.74, 151.00, 137.21, 134.93, 133.07, 129.10, 128.73 (×2), 128.37, 128.22, 125.86, 124.77, 124.44, 123.30, 122.80, 119.78, 119.22, 115.57 (×2), 113.34, 109.82, 68.17, 66.26, 62.44, 43.68, 39.41, 36.60, 33.73, 29.68, 22.54, 20.48; HRMS (ESI) *m/z* calcd for $C_{35}H_{33}N_3NaO_4S_3$ $[M+Na]^+$ 678.1525, found 678.1465.

*4.1.2.11 Compound* ***11a***. Brownish red solid, yield: 38%. $^1$H NMR ($CDCl_3$, 600 MHz) $\delta$ (ppm): 8.12 (d, *J* = 7.8 Hz, 1H, Ar-H), 7.61 (d, *J* = 7.8 Hz, 1H, Ar-H), 7.56 (d, *J* = 8.8 Hz, 2H, Ar-H), 7.45 (m, 1H, Ar-H), 7.39 (s, 1H, 4*H*-1,2-dithiole-3-thione), 7.25(m, 1H, Ar-H), 7.24 (m, 1H, Ar-H), 7.22 (m, 1H, Ar-H), 7.19 (m, 1H, Ar-H), 7.14 (m, 1H, Ar-H), 6.79 (d, *J* = 8.8 Hz, 2H, Ar-H), 5.91 (s, 1H, N-CH-N), 5.21 (m, 1H, 13-N-$CH_2$), 4.97 (m, 1H, 13-N-$CH_2$), 4.89 (m, 1H, N-$CH_2$), 4.35 m, 2H, O-$CH_2$-$CH_2$-O), 3.83 (m, 2H, O-$CH_2$-$CH_2$-O), 3.17 (m, 1H, N-$CH_2$), 2.97 (m, 1H, -$CH_2$), 2.87 (m, 1H, -$CH_2$), 2.37 (s, 3H, N-$CH_3$), 2.07 (m, 2H, -$CH_2$); $^{13}$C NMR ($CDCl_3$, 150 MHz) $\delta$ (ppm): 215.23, 172.97, 168.65, 164.52, 161.92, 150.87, 137.84, 134.80, 133.07, 129.12, 128.67 (×2), 128.14, 126.08, 124.81, 124.45, 123.52, 123.35, 120.46, 119.36, 115.42 (×2), 115.19, 114.20, 109.15, 68.07, 64.22, 62.04, 45.43, 39.31, 36.81, 28.34, 20.30; HRMS (ESI) *m/z* calcd for $C_{33}H_{29}N_3NaO_4S_3$ $[M+Na]^+$ 650.1212, found 650.1160.

*4.1.2.12 Compound* ***11b***. Brownish red solid, yield: 26%. $^1$H NMR ($CDCl_3$, 600 MHz) $\delta$ (ppm): 8.14 (dd, *J* = 7.8, 1.4 Hz, 1H, Ar-H), 7.61 (d, *J* = 7.8 Hz, 1H, Ar-H),

7.56 (d, *J* = 8.8 Hz, 2H, Ar-H), 7.49 (m, 1H, Ar-H), 7.43 (m, 1H, Ar-H), 7.36 (s, 1H, 4*H*-1,2-dithiole-3-thione), 7.28 (m, 1H, Ar-H), 7.23 (m, 1H, Ar-H), 7.19 (m, 1H, Ar-H), 7.16 (m, 1H, Ar-H), 6.92 (d, *J* = 8.8 Hz, 2H, Ar-H), 5.95 (s, 1H, N-CH-N), 4.90 (m, 1H, N-$CH_2$), 4.43 (m, 1H, O-$CH_2$-$CH_2$-O), 4.24 (m, 2H, O-$CH_2$-$CH_2$-O), 4.14 (m, 1H, O-$CH_2$-$CH_2$-O), 4.02 (m, 2H, 13-N-$CH_2$), 3.17 (m, 1H, N-$CH_2$), 3.02(m, 1H, -$CH_2$), 2.88 (m, 1H, -$CH_2$), 2.38 (s, 3H, N-$CH_3$), 2.35 (m, 2H, -$CH_2$), 2.16 (m, 2H, -$CH_2$), 2.04 (m, 2H, -$CH_2$); $^{13}$C NMR ($CDCl_3$, 150 MHz) $\delta$ (ppm): 215.16, 172.99, 172.68, 164.62, 162.09, 150.94, 137.30, 134.73, 133.02, 129.05, 128.68 (×2), 128.29, 128.15, 125.82, 124.41, 124.19, 123.26, 122.90, 119.84, 119.17, 115.46 (×2), 113.52, 109.84, 68.08, 64.79, 61.32, 43.00, 39.35, 36.53, 31.43, 28.42, 25.27, 20.44; HRMS (ESI) *m/z* calcd for $C_{35}H_{33}N_3NaO_4S_3$ $[M+Na]^+$ 678.1525, found 678.1458.

*4.1.2.13 Compound* ***11c***. Brownish red solid, yield: 14%. $^1$H NMR ($CDCl_3$, 600 MHz) $\delta$ (ppm): 8.14 (dd, *J* = 7.8, 1.4 Hz, 1H, Ar-H), 7.60 (m, 1H, Ar-H), 7.56 (d, *J* = 8.8 Hz, 2H, Ar-H), 7.49 (m, 1H, Ar-H), 7.39 (m, 1H, Ar-H), 7.37 (s, 1H, 4*H*-1,2-dithiole-3-thione), 7.28 (m, 1H, Ar-H), 7.23 (m, 1H, Ar-H), 7.21 (m, 1H, Ar-H), 7.17 (m, 1H, Ar-H), 6.91 (d, *J* = 8.8 Hz, 2H, Ar-H), 5.95 (s, 1H, N-CH-N), 4.90 (m, 1H, N-$CH_2$), 4.38 (m, 1H, O-$CH_2$-$CH_2$-O), 4.23 (m, 2H, O-$CH_2$-$CH_2$-O), 4.18 (m, 1H, O-$CH_2$-$CH_2$-O), 4.04 (m, 2H, 13-N-$CH_2$), 3.17 (m, 1H, N-$CH_2$), 3.02(m, 1H, -$CH_2$), 2.88 (m, 1H, -$CH_2$), 2.37 (s, 3H, N-$CH_3$), 2.34 (m, 2H, -$CH_2$), 2.08 (m, 2H, -$CH_2$), 1.86 (m, 2H, -$CH_2$), 1.70 (m, 2H, -$CH_2$); $^{13}$C NMR ($CDCl_3$, 150 MHz) $\delta$ (ppm): 215.24, 173.13, 173.01, 164.66, 162.13, 151.00, 137.20, 134.80, 133.07, 131.05, 129.10, 128.70 (×2), 128.37, 128.17, 125.86, 124.43, 123.28, 122.79, 119.77, 119.22, 115.49 (×2), 113.32, 109.80, 68.16, 64.81, 61.11, 43.69, 39.41, 36.59, 33.82, 30.68, 28.53, 22.58, 20.47; HRMS (ESI) *m/z* calcd for $C_{36}H_{35}N_3HO_4S_3$ $[M+H]^+$ 670.1862, found 670.1860.

*4.1.2.14 Compound* ***12a***. Brownish red solid, yield: 34%. $^{1}$H NMR ($CDCl_3$, 600 MHz) $\delta$ (ppm): 8.13 (dd, *J* = 7.8, 1.2 Hz, 1H, Ar-H), 7.61 (d, *J* = 7.8 Hz, 1H, Ar-H), 7.58 (d, *J* = 8.8 Hz, 2H, Ar-H), 7.48 (m, 1H, Ar-H), 7.38 (s, 1H, 4*H*-1,2-dithiole-3-thione), 7.29 (m, 2H, Ar-H), 7.24 (m, 1H, Ar-H), 7.20 (m, 1H, Ar-H), 7.17 (m, 1H, Ar-H), 6.89 (d, *J* = 8.8 Hz, 2H, Ar-H), 5.94 (s, 1H, N-CH-N), 5.20 (m, 1H, 13-N-$CH_2$), 4.97 (m, 1H, 13-N-$CH_2$), 4.90 (m, 1H, N-$CH_2$), 4.22 (m, 2H, O-$CH_2$-$CH_2$-O), 3.91 (m, 2H, O-$CH_2$-$CH_2$-O), 3.23 (m, 1H, N-$CH_2$), 3.02 (m, 1H, -$CH_2$), 2.89 (m, 1H, -$CH_2$), 2.41 (s, 3H, N-$CH_3$), 1.71–1.81 (m, 4H, -$CH_2$); $^{13}$C NMR ($CDCl_3$, 150 MHz) $\delta$ (ppm): 215.18, 173.08, 168.79, 164.56, 162.23, 150.91, 137.87, 134.72, 133.03, 129.10, 128.69 (×2), 128.16, 126.09, 124.74, 124.28, 123.51, 123.30, 120.41, 119.33, 115.45 (×2), 115.21, 114.17, 109.17, 68.09, 67.56, 65.10, 45.37, 39.34, 36.83, 29.80, 25.40, 20.31; HRMS (ESI) *m/z* calcd for $C_{34}H_{31}N_3NaO_4S_3$ $[M+Na]^+$ 664.1369, found 664.1388.

*4.1.2.15 Compound* ***12b***. Brownish red solid, yield: 10%. $^{1}$H NMR ($CDCl_3$, 600 MHz) $\delta$ (ppm): 8.14 (dd, *J* = 7.8, 1.4 Hz, 1H, Ar-H), 7.61 (d, *J* = 7.8 Hz, 1H, Ar-H), 7.58 (d, *J* = 8.8 Hz, 2H, Ar-H), 7.49 (m, 1H, Ar-H), 7.43 (m, 1H, Ar-H), 7.38 (s, 1H, 4*H*-1,2-dithiole-3-thione), 7.29 (m, 1H, Ar-H), 7.24 (m, 1H, Ar-H), 7.20 (m, 1H, Ar-H), 7.17 (m, 1H, Ar-H), 6.93 (d, *J* = 8.8 Hz, 2H, Ar-H), 5.96 (s, 1H, N-CH-N), 4.90 (m, 1H, N-$CH_2$), 4.45 (m, 1H, O-$CH_2$-$CH_2$-O), 4.26 (m, 1H, O-$CH_2$-$CH_2$-O), 4.10 (m, 1H, O-$CH_2$-$CH_2$-O), 4.02 (m, 1H, O-$CH_2$-$CH_2$-O), 3.99 (m, 2H, 13-N-$CH_2$), 3.19 (m, 1H, N-$CH_2$), 3.03 (m, 1H, -$CH_2$), 2.89 (m, 1H, -$CH_2$), 2.39 (s, 3H, N-$CH_3$), 2.36 (m, 2H, -$CH_2$), 2.17 (m, 2H, -$CH_2$), 1.81 (m, 2H, -$CH_2$), 1.75 (m, 2H, -$CH_2$); $^{13}$C NMR ($CDCl_3$, 150 MHz) $\delta$ (ppm): 215.24, 173.12, 172.80, 164.66, 162.33, 150.98, 137.35, 134.75, 133.04, 129.10, 128.72 (×2), 128.34, 128.18, 125.86, 124.43, 124.29, 123.29, 122.93, 119.86, 119.19, 115.50 (×2), 113.55, 109.88, 68.12, 67.76, 64.27,

43.07, 39.39, 36.57, 31.51, 25.77, 25.40, 25.34, 20.48. HRMS (ESI) *m/z* calcd for $C_{36}H_{35}N_3NaO_4S_3$ $[M+Na]^+$ 692.1682, found 692.1617.

*4.1.2.16 Compound* ***12c***. Brownish red solid, yield: 5%. $^1$H NMR ($CDCl_3$, 600 MHz) $\delta$ (ppm): 8.14 (dd, *J* = 7.8, 1.4 Hz, 1H, Ar-H), 7.60 (d, *J* = 7.8 Hz, 1H, Ar-H), 7.59 (d, *J* = 8.8 Hz, 2H, Ar-H), 7.50 (m, 1H, Ar-H), 7.38 (s, 1H, 4*H*-1,2-dithiole-3-thione), 7.37 (m, 1H, Ar-H), 7.28 (m, 1H, Ar-H), 7.24 (m, 1H, Ar-H), 7.22 (m, 1H, Ar-H), 7.17 (m, 1H, Ar-H), 6.93 (d, *J* = 8.8 Hz, 2H, Ar-H), 5.96 (s, 1H, N-CH-N), 4.90 (m, 1H, N-$CH_2$), 4.39 (m, 1H, O-$CH_2$-$CH_2$-O), 4.20 (m, 1H, O-$CH_2$-$CH_2$-O), 4.11 (m, 2H, O-$CH_2$-$CH_2$-O), 4.01 (m, 2H, 13-N-$CH_2$), 3.18 (m, 1H, N-$CH_2$), 3.02(m, 1H, -$CH_2$), 2.88 (m, 1H, -$CH_2$), 2.39 (s, 3H, N-$CH_3$), 2.33 (m, 2H, -$CH_2$), 1.76-1.90 (m, 8H, -$CH_2$); $^{13}$C NMR ($CDCl_3$, 150 MHz) $\delta$ (ppm): 215.26, 173.24, 173.13, 164.69, 162.36, 151.02, 137.22, 134.77, 133.08, 129.11, 128.73 (×2), 128.39, 128.19, 125.87, 124.44, 124.30, 123.30, 122.79, 119.76, 119.22, 115.51 (×2), 113.33, 109.83, 68.18, 67.78, 64.06, 43.70, 39.42, 36.61, 33.91, 29.77, 25.78, 25.47, 22.65, 20.49; HRMS (ESI) *m/z* calcd for $C_{37}H_{37}N_3HO_4S_3$ $[M+H]^+$ 684.2019, found 684.1935.

*4.2 MTT assay*

Antiproliferative activity was examined by the MTT assay following the method described previously [75,76]. The assay was performed in 96-well plates. Cells were added to each well and incubated for 24 h at 37 $^o$C in a humidified atmosphere of 5% $CO_2$. Then cells were incubated in the presence or absence of test compounds. After 72 h, MTT solution (20 $\mu$L/well, 5 mg/mL) was added to each cultured medium, which was incubated for another 4 h. DMSO (150 $\mu$L/well) was added to each well sequentially, 10 minutes of incubation at room temperature was followed. After 10 min, the OD of each well was measured on a Microplate Reader (BIO-RAD) at the

wavelength of 570 nm. In these experiments, the negative reference was 0.1% DMSO and 5-FU was used as the positive reference. The $IC_{50}$ values were calculated according to the inhibition ratios.

*4.3 Cell cycle analysis*

The cell cycle of HL-60 cell line treated with **12c** was evaluated by flow cytometry with PI (KGA511, KeyGEN Biotech, Nanjing, China). HL-60 cells were seeded in 6-well plates and incubated at 37 $^{o}$C for 24 h. Then, **12c** was dissolved in DMSO and added indicated concentrations for incubation in triplicate manner. Blank solvent of DMSO was added to control cells. After 48 h incubation, all cells were centrifuged and fixed in 70% ethanol at 4 $^{o}$C overnight and suspended again in PBS mixed with 100 $\mu$L RNase A and 400 $\mu$L PI. Cell cycle distribution of DNA content was assessed on a flow cytometer (FACS Calibur Becton-Dickinson, Franklin Lake, NJ, USA) [77].

*4.4 Hoechst 333258 staining*

The nuclear morphological modifications were analyzed by fluorescent microscopy using Hoechst staining. In this experiment, HL-60 cells were seeded on 6-well plates, with 2 mL of medium. After 24 h of incubation, **12c** was added at indicated concentrations and cells were incubated again for a period of 48 h. Cells were harvested by mild trypsinization, collected by centrifugation and washed twice with PBS. Cells were then stained with 500 $\mu$L of Hoechst solution (2 mg/mL in PBS) (Keygen, Nanjing, China) for 15 min at room temperature, in darkness. After incubation, cells were washed with PBS, mounted in a slide and observed with a fluorescent microscope with a DAPI filter [78].

*4.5 Cell apoptosis assay*

Apoptosis was analyzed using Annexin V and PI double staining by flow

cytometry according to the manufacturer's instructions (KGA1024, KeyGEN Biotech, Nanjing, China) in order to detect apoptotic cells. The HL-60 cells were seeded in 6-well plates overnight, then different concentrations of **12c** dissolved in DMSO were added in triplicate for 24 h incubation. After that, PBS was used twice to wash incubated cells, then resuspended in annexin V binding buffer. Annexin V-FITC was added to the mixture before 15 minutes incubation in total dark at 25 $^{o}$C. PI was applied right before acquisition. The percentage of cells positive for PI and/or Annexin V-FITC was reported inside the quadrants [79,80].

*4.6 Mitochondrial membrane potential assay*

HL-60 cells were incubated with target molecule **12c** (0.3, 0.6 and 1.2 $\mu$M) or vehicle solvent briefly in triplicate fashion for 48 h, then washed with PBS and stained with JC-1 dye under dark conditions according to the manufacturer's instructions (KeyGen Biotech, KGA601). The percentage shares of cells with healthy or collapsed mitochondrial membrane potentials were monitored through flow cytometry analysis [81].

*4.7 Western blot assay*

HL-60 cells were incubated with indicated doses (0.3, 0.6 and 1.*2* $\mu$M) of **12c** in triplicate for 72 h. The cells were harvested and lysed using lysis buffer, and the solution was centrifuged for 10 min at 4 $^{o}$C. After determination of protein concentrations, individual cell lysates were separated by sodium dodecyl sulfate polyacrylamide gel electrophoresis (10% gel, SDS-PAGE) and transferred onto nitrocellulose membranes. Target proteins in the membranes were blocked with 5% fat-free milk, and probed with monoclonal antibodies against Bcl-2, Bax, cytochrome *c*, caspase-9, -3, p53, cyclin B1, cdc2 and GAPDH (KeyGEN Biotech, Nanjing, China) at 4 $^{o}$C overnight, respectively. The bound antibodies were detected by appropriate

second antibodies and visualized using an enhanced chemiluminescent reagent. The relative optical densities of each protein to control GAPDH were determined by densimetric scanning [82].

**Acknowledgment**

This paper was financially supported by the Project Funded by China Post Doctoral Science Foundation (2017T100186), Natural Science Foundation of Liaoning Province (20170540858), General Scientific Research Projects of Department of Education in Liaoning Province (2017LQN05), and Career Development Support Plan for Young and Middle-aged Teachers in Shenyang Pharmaceutical University.

**References**

[1] J. Jiang, C. Hu, Evodiamine: a novel anti-cancer alkaloid from *Evodia rutaecarpa*, Molecules 14 (2009) 1852–1859.

[2] G. Huang, B. Kling, F.H. Darras, J. Heilmann, M. Decker, Identification of a neuroprotective and selective butyrylcholinesterase inhibitor derived from the natural alkaloid evodiamine, Eur. J. Med. Chem. 81 (2014) 15–21.

[3] Y.N. Zhang, Y.F. Yang, X.W. Yang, Blood-brain barrier permeability and neuroprotective effects of three main alkaloids from the fruits of *Euodia rutaecarpa* with MDCK-pHaMDR cell monolayer and PC12 cell line, Biomed. Pharmacother. 98 (2018) 82–87.

[4] J. Yang, X.T. Cai, W.G. Lu, C.P. Hu, X.J. Xu, Q. Yu, P. Cao, Evodiamine inhibits STAT3 signaling by inducing phosphatase shatterproof 1 in hepatocellular carcinoma cells, Cancer Lett. 328 (2013) 243–251.

[5] Y.T. Zhang, Z. Li, K. Zhang, H.Y. Zhang, Z.H. He, Q. Xia, J.H. Zhao, N.P Feng, Co-delivery of evodiamine and rutaecarpine in a microemulsion-based hyaluronic acid hydrogel for enhanced analgesic effects on mouse pain models, Int. J. Pharm. 528 (2017) 1–2.

[6] Y. Hu, H. Fahmy, J.K. Zjawiony, G.E. Davies, Inhibitory effect and transcriptional impact of berberine and evodiamine on human white preadipocyte differentiation, Fitoterapia 81 (2010) 259–268.

[7] X. Zhou, F. Ren, H. Wei, L. Liu, T. Shen, S. Xu, J. Wei, J. Ren, H. Ni, Combination of berberine and evodiamine inhibits intestinal cholesterol absorption in high fat diet induced hyperlipidemic rats, Lipids Health Dis. 16 (2017) 239.

[8] X. Fan, J.Y. Zhu, Y. Sun, L. Luo. J. Yan, X. Yang, J. Yu, W.Q. Tang, W. Ma, H.P. Liang, Evodiamine inhibits zymosan-induced inflammation *in vitro* and *in vivo*: inactivation of NF-$\kappa$B by inhibiting I$\kappa$B$\alpha$ phosphorylation, Inflammation 40 (2017) 1012–1027.

[9] L. Jiang, X. Zhao, J. Pei, L. Mei, Y. Cui, S. Wang, Y. Shao, X. Zhang, Y. Tao, Daily chemical evodiamine from Chinese prickly ash attenuates osteoclast differentiation through RANKL induced NFAT pathways, J. Funct. Foods 37 (2017) 594–602.

[10] Y.H. Ko, K.Y. Shim, S.Y. Lee, C.G. Jiang, Evodiamine reduces caffeine-induced sleep disturbances and excitation in mice, Biomol. Ther. (2018) 1–7.

[11] D. Yang, L. Li, S. Qian, L. Liu, Evodiamine ameliorates liver fibrosis in rats via TGF-$\beta$1/Smad signaling pathway, J. Nat. Med. 72 (2018) 145–154.

[12] Q.Q. Wu, Y. Xiao, X.H. Jiang, Y. Yuan, Z. Yang, W. Chang, Z.Y. Bian, Q.Z. Tang, Evodiamine attenuates TGF-$\beta$1-induced fbroblast activation and

endothelial to mesenchymal transition, Mol. Cell Biochem. 430 (2017) 89–91.

[13] N. He, Q.H. Gong, F. Zhang, J.Y. Zhang, S.X. Lin, H.H. Hou, Q. Wu, A.S. Sun, Evodiamine inhibits angiotensin □-induced rat cardiomyocyte hypertrophy, Chin. J. Integr. Med. (2017) doi: 10.1007/s11655-017-2818-9.

[14] S. Wang, K. Fang, G. Dong, S. Chen, N. Liu, Z. Miao, J. Yao, J. Li, W. Zhang, C. Sheng, Scaffold diversity inspired by the natural product evodiamine: discovery of highly potent and multitargeting antitumor agents, J. Med. Chem. 58 (2015) 6678–6696.

[15] G. Dong, S. Wang, Z. Miao, J. Yao, Y. Zhang, Z. Guo, W. Zhang, C. Sheng, New tricks for an old natural product: discovery of highly potent evodiamine derivatives as novel antitumor agents by systemic structure-activity relationship analysis and biological evaluations, J. Med. Chem. 55 (2012) 7593–7613.

[16] G. Dong, C. Sheng, S. Wang, Z. Miao, J. Yao, W. Zhang, Selection of evodiamine as a novel topoisomerase I inhibitor by structure-based virtual screening and hit optimization of evodiamine derivatives as antitumor agents, J. Med. Chem. 53 (2010) 7521–7531.

[17] Q. Tan, J. Zhang, Evodiamine and its role in chronic diseases, Adv. Exp. Med. Biol. 929 (2016) 315–328.

[18] F. Yang, L. Shi, T. Liang, L. Ji, G. Zhang, Y. Shen, F. Zhu, L. Xu, Anti-tumor effect of evodiamine by inducing Akt-mediated apoptosis in hepatocellular carcinoma, Biochem. Biophys. Res. Commun. 485 (2017) 54–61.

[19] C.S. Shi, J.M. Li, C.C. Chin, Y.H. Kuo, Y.R. Lee, Y.C. Huang, Evodiamine induces cell growth arrest, apoptosis and suppresses tumorigenesis in human urothelial cell carcinoma cells, Anticancer Res. 37 (2017) 1149–1159.

[20] X.L. Yuan, P. Zhang, X.M. Liu, Y.M. Du, X.D. Hou, S. Cheng, Z.F. Zhang,

Cytological assessments and transcriptome profling demonstrate that evodiamine inhibits growth and induces apoptosis in a renal carcinoma cell line, Sci. Rep. 7 (2017) 12572.

[21] Y. Zou, X. Qin, H. Xiong, F. Zhu, T. Chen, H. Wu, Apoptosis of human non-small-cell lung cancer A549 cells triggered by evodiamine through MTDH-dependent signaling pathway, Tumour Biol. 36 (2015) 5187–5193.

[22] X. Peng, Q. Zhang, Y. Zeng, J. Li, L. Wang, P. Ai, Evodiamine inhibits the migration and invasion of nasopharyngeal carcinoma cells in vitro via repressing MMP-2 expression, Cancer Chemother. Pharmacol. 76 (2015) 1173–1184.

[23] X. Pan, J.M. Hartley, J.A. Hartley, K.N. White, Z. Wang, S.W. Bligh, Evodiamine, a dual catalytic inhibitor of type I and II topoisomerases, exhibits enhanced inhibition against camptothecin resistant cells, Phytomedicine 19 (2012) 618–624.

[24] Z. Wen, S. Feng, L. Wei, Z. Wang, D. Hong, Q. Wang, Evodiamine, a novel inhibitor of the Wnt pathway, inhibits the self-renewal of gastric cancer stem cells, Int. J. Mol. Med. 36 (2015) 1657–1663.

[25] K. Sachita, Y. Kim, H.J. Yu, S.D. Cho, J.S. Lee, *In vitro* assessment of the anticancer potential of evodiamine in human oral cancer cell lines, Phytother. Res. 29 (2015) 1145–1151.

[26] L.C. Zhao, J. Li, K. Liao, N. Luo, Q.Q. Shi, Z.Q. Feng, D.L. Chen, Evodiamine induces apoptosis and inhibits migration of HCT-116 human colorectal cancer cells, Int. J. Mol. Sci. 16 (2015) 27411–27421.

[27] W.T. Wei, H. Chen, Z.H. Wang, Z.L. Ni, H.B. Liu, H.F. Tong, H.C. Guo, D.L. Liu, S.Z. Lin, Enhanced antitumor efficacy of gemcitabine by evodiamine on pancreatic cancer via regulating PI3K/Akt pathway, Int. J. Biol. Sci. 8 (2012)

1–14.

[28] T. Zhang, S. Qu, Q. Shi, D. He, X. Jin, Evodiamine induces apoptosis and enhances TRAIL-induced apoptosis in human bladder cancer cells through mTOR/S6K1-mediated downregulation of Mcl-1, Int. J. Mol. Sci. 15 (2014) 3154–3171.

[29] S. Wang, L. Wang, Z. Shi, Z. Zhong, M. Chen, Y. Wang, Evodiamine synergizes with doxorubicin in the treatment of chemoresistant human breast cancer without inhibiting p-glycoprotein, PLoS One 9 (2014) e97512.

[30] Z.F. Zhong, W. Tan, S.P. Wang, W.A. Qiang, Y.T. Wang, Anti-proliferative activity and cell cycle arrest induced by evodiamine on paclitaxel-sensitive and -resistant human ovarian cancer cells, Sci. Rep. 5 (2015) 16415.

[31] C.Y. Hu, H.T. Wu, Y.C. Su, C.H. Lin, C.J. Chang, C.L. Wu, Evodiamine exerts an anti-Hepatocellular carcinoma activity through a WWOX-dependent pathway, Molecules 22 (2017) E1175.

[32] C. Huang, H. Liu, X.L. Gong, L.Y. Wu, B. Wen, Effect of evodiamine and berberine on the interaction between DNMTs and target microRNAs during malignant transformation of the colon by TGF-β1, Oncol. Rep. 37 (2017) 1637–1645.

[33] C. Szabo, A. Papapetropoulos, International union of basic and clinical pharmacology. CII: pharmacological modulation of $H_2S$ levels: $H_2S$ donors and $H_2S$ biosynthesis inhibitors, Pharmacol. Rev. 69 (2017) 497–564.

[34] J.L. Wallace, R. Wang, Hydrogen sulfide-based therapeutics: exploiting a unique but ubiquitous gasotransmitter, Nat. Rev. Drug Discov. 14 (2015) 329–345.

[35] D. Wu, J. Wang, H. Li, M. Xue, A. Ji, Y. Li, Role of hydrogen sulfide in ischemia-reperfusion injury, Oxid. Med. Cell Longev. 2015 (2015) 186908.

[36] L. Xiao, J.H. Dong, X. Teng, S. Jin, H.M. Xue, S.Y. Liu, Q. Guo, W. Shen, X.C. Ni, Y.M. Wu, Hydrogen sulfide improves endothelial dysfunction in hypertension by activating peroxisome proliferator-activated receptor delta/endothelial nitric oxide synthase signaling, J. Hypertens. 36 (2018) 651–665.

[37] S. Mani, A. Untereiner, L. Wu, R. Wang, Hydrogen sulfide and the pathogenesis of atherosclerosis, Antioxid. Redox Signal. 20 (2014) 805–817.

[38] Y.Y. Mok, M.S. Atan, C.Y. Ping, W.Z. Jing, M. Bhatia, S. Moochhala, P.K. Moore, Role of hydrogen sulphide in haemorrhagic shock in the rat: protective effect of inhibitors of hydrogen sulphide biosynthesis, Br. J. Pharmacol. 143 (2004) 881–889.

[39] N. Sen, Functional and molecular insights of hydrogen sulfide signaling and protein sulfhydration, J. Mol. Biol. 429 (2017) 543–561.

[40] R.N. Carter, N.M. Morton, Cysteine and hydrogen sulphide in the regulation of metabolism: insights from genetics and pharmacology, J. Pathol. 238 (2016) 321–332.

[41] C. Szabo, Gasotransmitters in cancer: from pathophysiology to experimental therapy, Nat. Rev. Drug Discov. 15 (2016) 185–203.

[42] M.R. Hellmich, C. Szabo, Hydrogen sulfide and cancer, Handb. Exp. Pharmacol. 230 (2015) 233–241.

[43] N. Sen, B.D Paul, M.M. Gadalla, A.K. Mustafa, T. Sen, R. Xu, S. Kim, S.H. Snyder, Hydrogen sulfide-linked sulfhydration of NF-$\kappa$B mediates its anti-apoptotic actions, Mol. Cell 45 (2012) 13–24.

[44] F. Sekiguchi, T. Sekimoto, A. Ogura, A. Kawabata, Endogenous hydrogen sulfide enhances cell proliferation of human gastric cancer AGS cells, Biol. Pharm. Bull. 39 (2016) 887–890.

[45] D. Wu, M. Li, W. Tian, S. Wang, L. Cui, H. Li, H. Wang, A. Ji, Y. Li, Hydrogen sulfide acts as a double-edged sword in human hepatocellular carcinoma cells through EGFR/ERK/MMP-2 and PTEN/AKT signaling pathways, Sci. Rep. 7 (2017) 5134.

[46] S.S. Wang, Y.H. Chen, N. Chen, L.J. Wang, D.X. Chen, H.L. Weng, S. Dooley, H.G. Ding, Hydrogen sulfide promotes autophagy of hepatocellular carcinoma cells through the PI3K/Akt/mTOR signaling pathway, Cell Death Dis. 8 (2017) e2688.

[47] Y. Zhen, W. Zhang, C. Liu, J. He, Y. Lu, R. Guo, J. Feng, Y. Zhang, J. Chen, Exogenous hydrogen sulfde promotes C6 glioma cell growth through activation of the p38 MAPK/ERK1/2-COX-2 pathways, Oncol. Rep. 34 (2015) 2413–2422.

[48] Y. Zhao, T.D. Biggs, M. Xian, Hydrogen sulfide ($H_2S$) releasing agents: chemistry and biological applications, Chem. Commun. 50 (2014) 11788–11805.

[49] C.R. Powell, K.M. Dillon, J.B. Matson, A review of hydrogen sulfide ($H_2S$) donors: Chemistry and potential therapeutic applications, Biochem. Pharmacol. (2017) doi: 10.1016/j.bcp.2017.11.014.

[50] Z.W. Lee, J. Zhou, C.S. Chen, Y. Zhao, C.H. Tan, L. Li, P.K. Moore, L.W. Deng, The slow-releasing hydrogen sulfide donor, GYY4137, exhibits novel anti-cancer effects *in vitro* and *in vivo*, PLoS One 6 (2011) e21077.

[51] S. Lu, Y. Gao, X. Huang, X. Wang, GYY4137, a hydrogen sulfide ($H_2S$) donor, shows potent anti-hepatocellular carcinoma activity through blocking the STAT3 pathway, Int. J. Oncol. 44 (2014) 1259–1267.

[52] J. Frantzias, J.G. Logan, P. Mollat, A. Sparatore, P. Del Soldato, S.H. Ralston, A.I. Idris, Hydrogen sulphide-releasing diclofenac derivatives inhibit breast cancer-induced osteoclastogenesis *in vitro* and prevent osteolysis *ex vivo*, Br. J.

Pharmacol. 165 (2012) 1914–1925.

[53] K. Chegaev, B. Rolando, D. Cortese, E. Gazzano, I. Buondonno, L. Lazzarato, M. Fanelli, C.M. Hattinger, M. Serra, C. Riganti, R. Fruttero, D. Ghigo, A. Gasco, $H_2S$-donating doxorubicins may overcome cardiotoxicity and multidrug resistance, J. Med. Chem. 59 (2016) 4881–4889.

[54] W. Feng, X.Y. Teo, W. Novera, P.M. Ramanujulu, D. Liang, D. Huang, P.K. Moore, L.W. Deng, B.W. Dymock, Discovery of new $H_2S$ releasing phosphordithioates and 2,3-dihydro-2-phenyl-2-sulfanylenebenzo[*d*][1,3,2]oxazaphospholes with improved antiproliferative activity, J. Med. Chem. 58 (2015) 6456–6480.

[55] C.T. Yang, L. Chen, S. Xu, J.J. Day, X. Li, M. Xian, Recent development of hydrogen sulfide releasing/stimulating reagents and their potential applications in cancer and glycometabolic disorders, Front Pharmacol. 8 (2017) 664.

[56] P.D. Cicco, E. Panza, G. Ercolano, C. Armogida, G. Sessa, G. Pirozzi, G. Cirino, J.L. Wallace, A. Ianaro, ATB-346, a novel hydrogen sulfide-releasing anti-inflammatory drug, induces apoptosis of human melanoma cells and inhibits melanoma development *in vivo*, Pharmacol. Res. 114 (2016) 67–73.

[57] A. Ianaro, G. Cirino, J.L. Wallace, Hydrogen sulfide-releasing anti-inflammatory drugs for chemoprevention and treatment of cancer, Pharmacol. Res. 111 (2016) 652–658.

[58] U. Hasegawa, N. Tateishi, H. Uyama, A.J. van der Vlies, Hydrolysis-sensitive dithiolethione prodrug micelles, Macromol. Biosci. 15 (2015) 1512–1522.

[59] M. Li, J. Li, T. Zhang, Q. Zhao, J. Cheng, B. Liu, Z. Wang, L. Zhao, C. Wang, Syntheses, toxicities and anti-inflammation of $H_2S$-donors based on non-steroidal anti-inflammatory drugs, Eur. J. Med. Chem. 138 (2017) 51–65.

[60] Y. Zhao, H. Wang, M. Xian, Cysteine-activated hydrogen sulfide ($H_2S$) donors, J. Am. Chem. Soc. 133 (2011) 15–17.

[61] E. Barresi, G. Nesi, V. Citi, E. Piragine, I. Piano, S. Taliani,F. Da Settimo, S. Rapposelli, L. Testai, M.C. Breschi, C. Gargini, V. Calderone, A. Martelli, Iminothioethers as hydrogen sulfide donors: from the gasotransmitter release to the vascular effects, J. Med. Chem. 60 (2017) 7512–7523.

[62] J. Kang, A.J. Ferrell, W. Chen, D. Wang, M. Xian, Cyclic acyl disulfides and acyl selenylsulfides as the precursors for persulfides (RSSH), selenylsulfides (RSeSH), and hydrogen sulfide ($H_2S$), Org. Lett. 20 (2018) 852–855.

[63] M.M. Cerda, M.D. Hammers, M.S. Earp, L.N. Zakharov, M.D. Pluth, Applications of synthetic organic tetrasulfides as $H_2S$ donors, Org. Lett. 19 (2017) 2314–2317.

[64] B. Severino, A. Corvino, F. Fiorino, P. Luciano, F. Frecentese, E. Magli, I. Saccone, P. Di Vaio, V. Citi, V. Calderone, L. Servillo, R. Casale, G. Cirino, V. Vellecco, M. Bucci, E. Perissutti, V. Santagada, G. Caliendo, 1,2,4-thiadiazolidin-3,5-diones as novel hydrogen sulfide donors, Eur. J. Med. Chem. 143 (2018) 1677–1686.

[65] N. Zhao, K.T. Tian, K.G. Cheng, T. Han, X. Hu, D.H. Li, Z.L. Li, H.M. Hua, Antiproliferative activity and apoptosis inducing effects of nitric oxide donating derivatives of evodiamine, Bioorg. Med. Chem. 24 (2016) 2971–2978.

[66] X. Hu, Y. Wang, J. Xue, T. Han, R. Jiao, Z. Li, W. Liu, F. Xu, H. Hua, D. Li, Design and synthesis of novel nitrogen mustard-evodiamine hybrids with selective antiproliferative activity, Bioorg. Med. Chem. Lett. 27 (2017) 4989–4993.

[67] B.M.F. Gonçalves, J.A.R. Salvador, S. Marín, M. Cascante, Synthesis and

anticancer activity of novel fluorinated asiatic acid derivatives, Eur. J. Med. Chem. 114 (2016) 101–117.

[68] S. Kasibhatla, B. Tseng, Why target apoptosis in cancer treatment? Mol. Cancer Ther. 2 (2003) 573–580.

[69] M. Loeffler, G. Kroemer, The mitochondrion in cell death control: Certainties and incognita, Exp. Cell Res. 256 (2000) 19–26.

[70] S. Ma, D. Zhong, P. Ma, G. Li, W. Hua, Y. Sun, N. Liu, L. Zhang, W. Zhang, Exogenous hydrogen sulfde ameliorates diabetes-associated cognitive decline by regulating the mitochondria-mediated apoptotic pathway and IL-23/IL-17 expression in db/db mice, Cell Physiol. Biochem. 41 (2017) 1838–1850.

[71] T.H. Wang, H.S. Wang, Y.K. Soong, Paclitaxel-induced cell death: where the cell cycle and apoptosis come together, Cancer 88 (2000) 2619–2628.

[72] S.A. Innocente, J.P. Cogswell, J.M. Lee, p53 regulates a $G_2$ checkpoint through cyclin B1, Proc. Natl. Acad. Sci. USA. 96 (1999) 2147–2152.

[73] S.F. Zheng, R.K. Bao, Q.J. Zhang, S.C. Wang, H.J. Lin, Endogenous hydrogen sulfide promotes apoptosis *via* mitochondrial pathways in the livers of broilers with selenium deficiency exudative diathesis disease, Biol. Trace Elem. Res. (2018) doi: 10.1007/s12011-018-1292-3.

[74] J.F.R. Kerr, A.H. Wyllie, A.R. Currie, Apoptosis: a basic biological phenomenon with wide-ranging implications in tissue kinetics, Br. J. Canc. 26 (1972) 239–257.

[75] K. Tian, F. Xu, X. Gao, T. Han, J. Li, H. Pan, L. Zang, D. Li, Z. Li, T. Uchita, M. Gao, H. Hua, Nitric oxide-releasing derivatives of brefeldin A as potent and highly selective anticancer agents, Eur. J. Med. Chem. 136 (2017) 131–143.

[76] T. Han, J. Li, J. Xue, H. Li, F. Xu, K. Cheng, D. Li, Z. Li, M. Gao, H. Hua, Scutellarin derivatives as apoptosis inducers: Design, synthesis and biological

evaluation, Eur. J. Med. Chem. 135 (2017) 270–281.

[77] X. Gao, J. Li, M. Wang, S. Xu, W. Liu, L. Zang, Z. Li, H. Hua, J. Xu, D. Li, Novel enmein-type diterpenoid hybrids coupled with nitrogen mustards: Synthesis of promising candidates for anticancer therapeutics, Eur. J. Med. Chem. 146 (2018) 588–598.

[78] J. Chen, T. Wang, S. Xu, A. Lin, H. Yao, W. Xie, Z. Zhu, J. Xu, Design, synthesis and biological evaluation of novel nitric oxide-donating protoberberine derivatives as antitumor agents, Eur. J. Med. Chem. 132 (2017) 173–183.

[79] S. Xu, H. Yao, S. Luo, Y.K. Zhang, D.H. Yang, D. Li, G. Wang, M. Hu, Y. Qiu, X. Wu, H. Yao, W. Xie, Z.S. Chen, J. Xu, A novel potent anticancer compound optimized from a natural oridonin scaffold induces apoptosis and cell cycle arrest through the mitochondrial pathway, J. Med. Chem. 60 (2017) 1449–1468.

[80] J. Chen, T. Wang, S. Xu, P. Zhang, A. Lin, L. Wu, H. Yao, W. Xie, Z. Zhu, J. Xu, Discovery of novel antitumor nitric oxide-donating $\beta$-elemene hybrids through inhibiting the PI3K/Akt pathway, Eur. J. Med. Chem. 135 (2017) 414–423.

[81] S. Xu, H. Yao, L. Pei, M. Hu, D. Li, Y. Qiu, G. Wang, L. Wu, H. Yao, Z. Zhu, J. Xu, Design, synthesis, and biological evaluation of NAD(P)H: Quinone oxidoreductase (NQO1)-targeted oridonin prodrugs possessing indolequinone moiety for hypoxia-selective activation, Eur. J. Med. Chem. 132 (2017) 310–321.

[82] T. Han, K. Tian, H. Pan, Y. Liu, F. Xu, Z. Li, T. Uchita, M. Gao, H. Hua, D. Li, Novel hybrids of brefeldin A and nitrogen mustards with improved antiproliferative selectivity: Design, synthesis and antitumor biological evaluation, Eur. J. Med. Chem. 150 (2018) 53–63.

**Table 1**

Antiproliferative activities of target compounds **8-12** against five human cancer cell lines and human normal peripheral blood mononuclear cells.

| Compound | $IC_{50}$ ($\mu$M)[a] | | | | | |
|---|---|---|---|---|---|---|
| | Bel-7402 | MCF-7 | SGC-7901 | Caco-2 | HL-60 | PBMC |
| **1** | 1.19 ± 0.06 | 28.53 ± 0.46 | 6.93 ± 1.05 | 2.73 ± 0.05 | 1.36 ± 0.07 | 20.96 ± 1.08 |
| **5** | > 50 | > 50 | > 50 | 35.47 ± 1.80 | 25.90 ± 1.59 | > 100 |
| **7** | > 50 | > 50 | > 50 | 14.28 ± 0.64 | 16.36 ± 1.24 | > 100 |
| **8a** | 20.53 ± 0.89 | 9.47 ± 0.38 | > 50 | 3.18 ± 0.17 | 0.97 ± 0.03 | > 100 |
| **8b** | > 50 | 39.74 ± 2.59 | > 50 | 2.84 ± 0.15 | 2.09 ± 0.07 | > 100 |
| **8c** | > 50 | 22.44 ± 0.35 | 31.03 ± 1.45 | 5.14 ± 0.18 | 9.38 ± 0.23 | > 100 |
| **8d** | 22.06 ± 1.41 | 27.98 ± 1.33 | 35.68 ± 1.86 | 4.88 ± 0.10 | 3.49 ± 0.09 | > 100 |
| **9a** | 25.83 ± 1.50 | 47.53 ± 1.40 | 26.76 ± 1.23 | 22.90 ± 1.43 | > 50 | > 100 |
| **9b** | > 50 | > 50 | > 50 | 4.08 ± 0.14 | 14.06 ± 1.01 | > 100 |
| **9c** | > 50 | 48.73 ± 1.27 | 30.22 ± 1.01 | 38.06 ± 1.75 | > 50 | > 100 |
| **10a** | 26.84 ± 2.06 | 38.40 ± 2.09 | 32.93 ± 1.78 | 6.35 ± 0.27 | 1.92 ± 0.08 | > 100 |
| **10b** | 45.24 ± 1.98 | 40.17 ± 1.72 | 47.35 ± 2.72 | 4.18 ± 0.03 | 1.03 ± 0.03 | > 100 |
| **10c** | 41.36 ± 2.38 | 29.65 ± 1.93 | 43.63 ± 1.91 | 4.22 ± 0.10 | 2.09 ± 0.11 | > 100 |
| **11a** | 34.25 ± 1.66 | 27.86 ± 1.02 | 24.74 ± 2.02 | 5.10 ± 0.11 | 2.74 ± 0.23 | > 100 |
| **11b** | > 50 | > 50 | > 50 | 2.81 ± 0.07 | 1.04 ± 0.07 | > 100 |
| **11c** | 30.54 ± 1.62 | > 50 | > 50 | 3.05 ± 0.06 | 0.99 ± 0.08 | > 100 |
| **12a** | > 50 | > 50 | > 50 | 4.34 ± 0.08 | 0.83 ± 0.05 | > 100 |
| **12b** | 45.03 ± 1.77 | 29.06 ± 2.01 | > 50 | 3.87 ± 0.05 | 0.70 ± 0.05 | > 100 |
| **12c** | 48.94 ± 2.40 | 44.82 ± 3.64 | > 50 | 2.02 ± 0.04 | 0.58 ± 0.02 | > 100 |
| **5-FU** | 18.97 ± 1.02 | 26.91 ± 1.35 | 19.84 ± 1.21 | 38.77 ± 1.48 | 3.46 ± 0.21 | NT[b] |

[a]$IC_{50}$: Half inhibitory concentrations measured by the MTT assay, the cells were incubated for 72 h. The values are expressed as averages ± standard deviations of three independent experiments. [b] NT: not tested.

**1. Legends of Fig. 1, Fig. 2, Fig. 3, Fig. 4, Fig. 5, Fig. 6, Scheme 1 and Scheme 2**

**Fig. 1.** Chemical structures of some reported $H_2S$ donating derivatives.

**Fig. 2.** Cell cycle arrest at $G_2$/M phase by **12c** in HL-60 cells. HL-60 cells were incubated with the indicated concentrations of **12c** for 48 h and the cells were stained with PI. Cellular DNA content, for cell cycle distribution analysis, was measured using a flow cytometry. The diagrams showed the distribution of the cells according to their DNA content. The inserts gave the percentages in different cell cycle phases.

**Fig. 3.** Hoechst staining of **12c** treated HL-60 cells. Cells were treated with the indicated concentrations of **12c** or vehicle for 48 h, stained with Hoechst 33258 and examined with a fluorescent microscope.

**Fig. 4.** Apoptosis in HL-60 cells by the treatment with **12c**. HL-60 cells were incubated with different concentrations of **12c** for 48 h and the cells were stained with annexin V-FITC and PI, followed by flow cytometry analysis.

**Fig. 5.** Effects of **12c** on the mitochondrial membrane potentials of HL-60 cells. HL-60 cells were incubated with the indicated concentrations of **12c** for 48 h prior to staining with JC-1.

**Fig. 6.** Western blot of apoptosis-related proteins in HL-60 cells after exposure to different concentrations of **12c** for 48 h.

**Scheme 1**. Synthesis of compounds **2a-d**, **4a-c** and **6a-c**. *Reagents and conditions*: (a) $HO(CH_2)_nBr$, NaH, anhydrous DMF, rt, 3 h; (b) $Br(CH_2)_nCOOC_2H_5$, NaH, anhydrous DMF, 80 □, 12 h; (c) potassium hydroxide, methanol, rt, 2 h; (d) $Br(CH_2)_nBr$, potassium carbonate, anhydrous acetone, reflux, 8 h.

**Scheme 2**. Synthesis of $H_2S$-releasing evodiamine derivatives **8-12**. *Reagents and conditions*: (a) *α*-thioctic acid, **5**, EDCI, DMAP, anhydrous DCM, rt, 8–12 h; (b) **6a-c**, TEA, anhydrous DMF, 80 □, 8 h.

**2. Graphics for Fig. 1, Fig. 2, Fig. 3, Fig. 4, Fig. 5, Fig. 6, Scheme 1 and Scheme 2**

**Fig. 1**

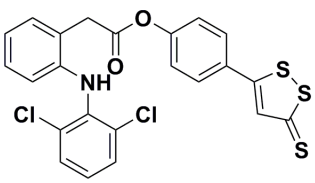


A

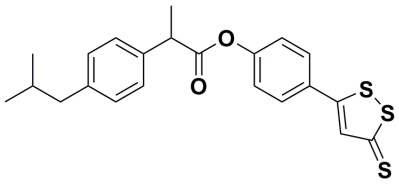


B

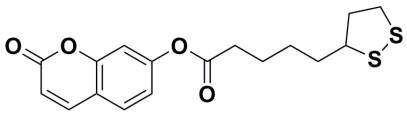


C

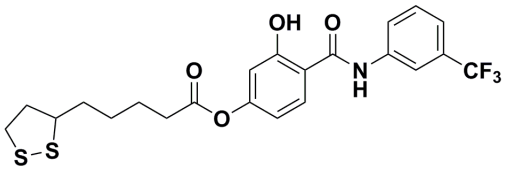


D

**Fig. 2**

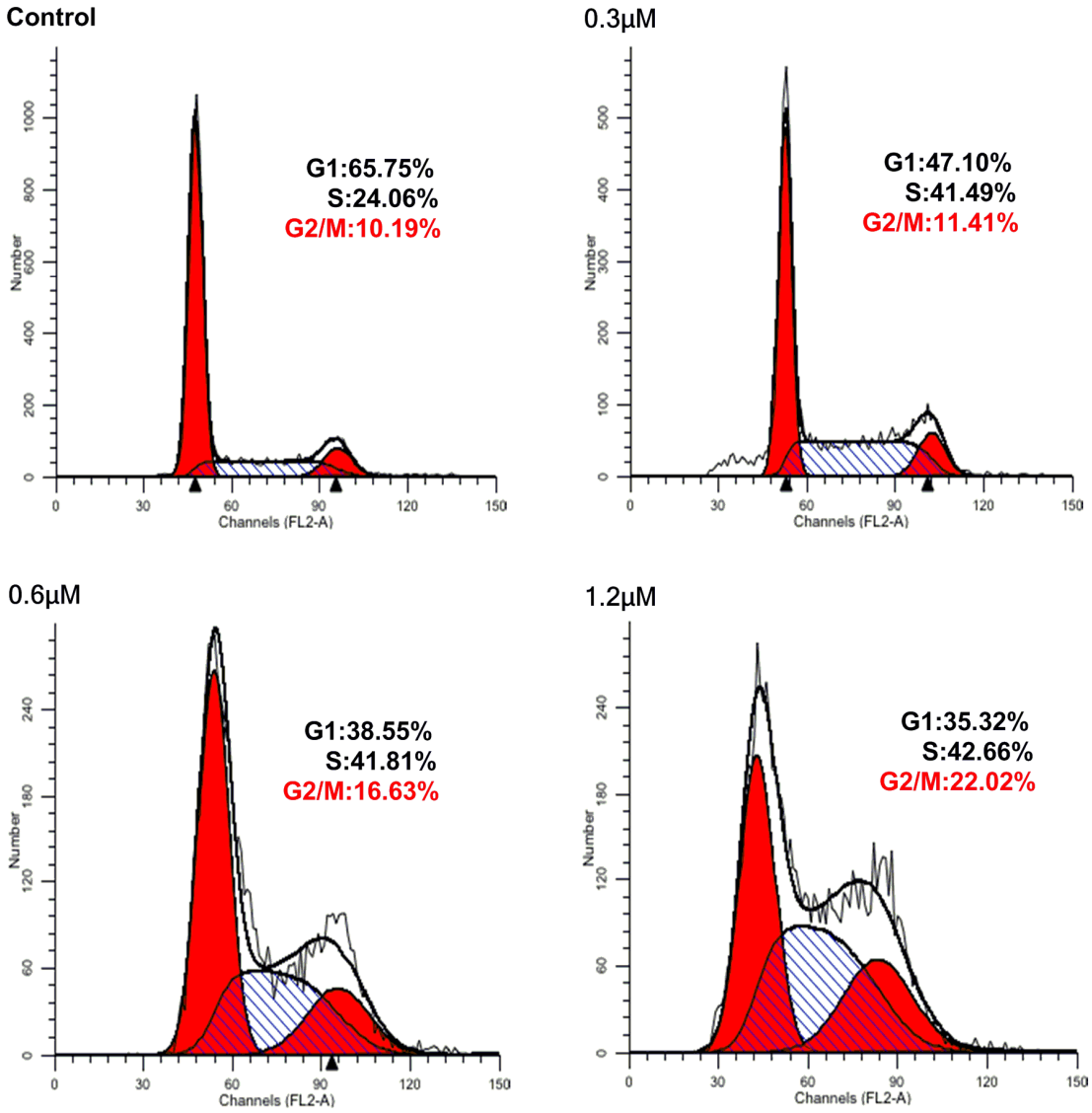

**Fig. 3**

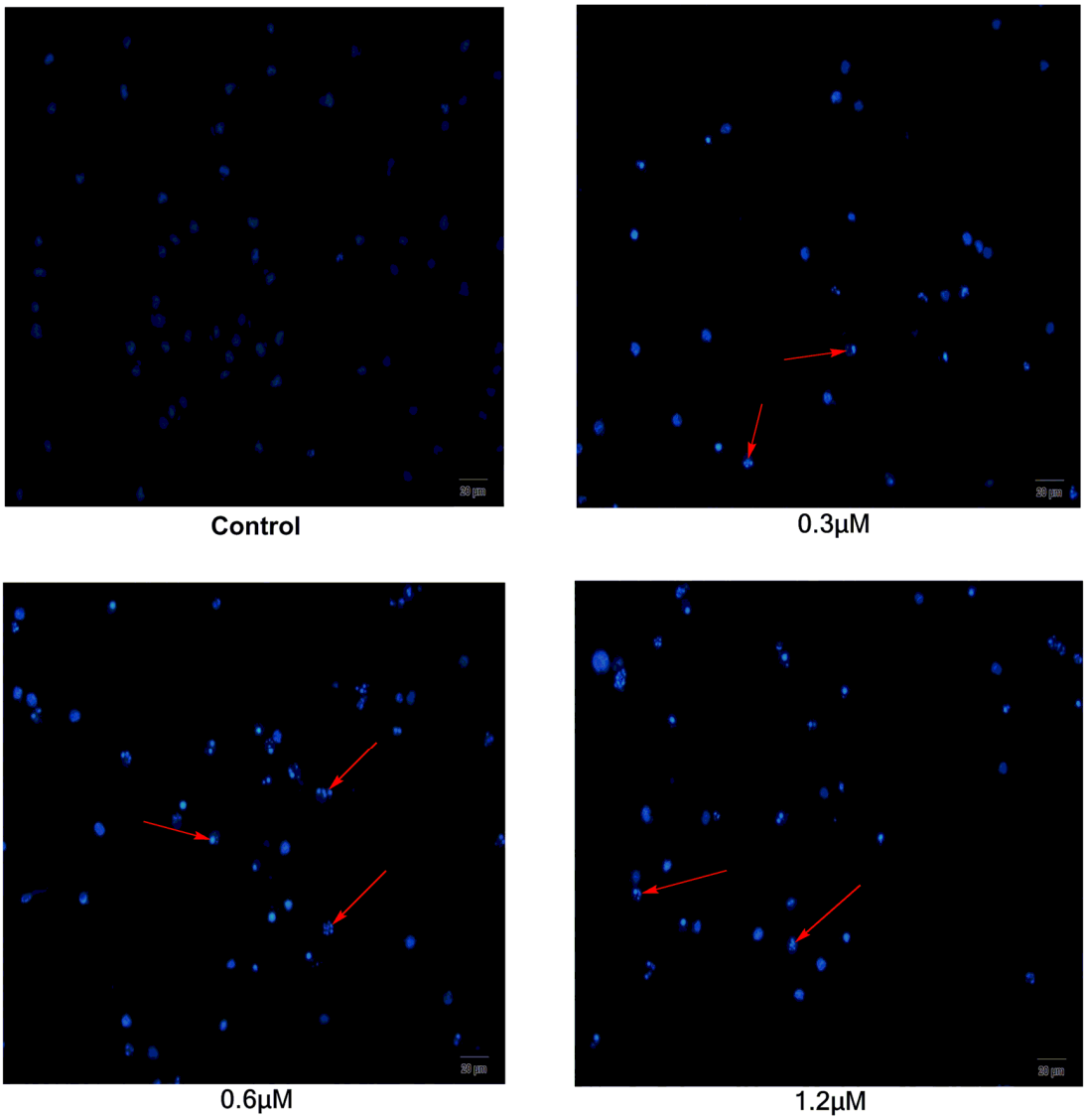

**Fig. 4**

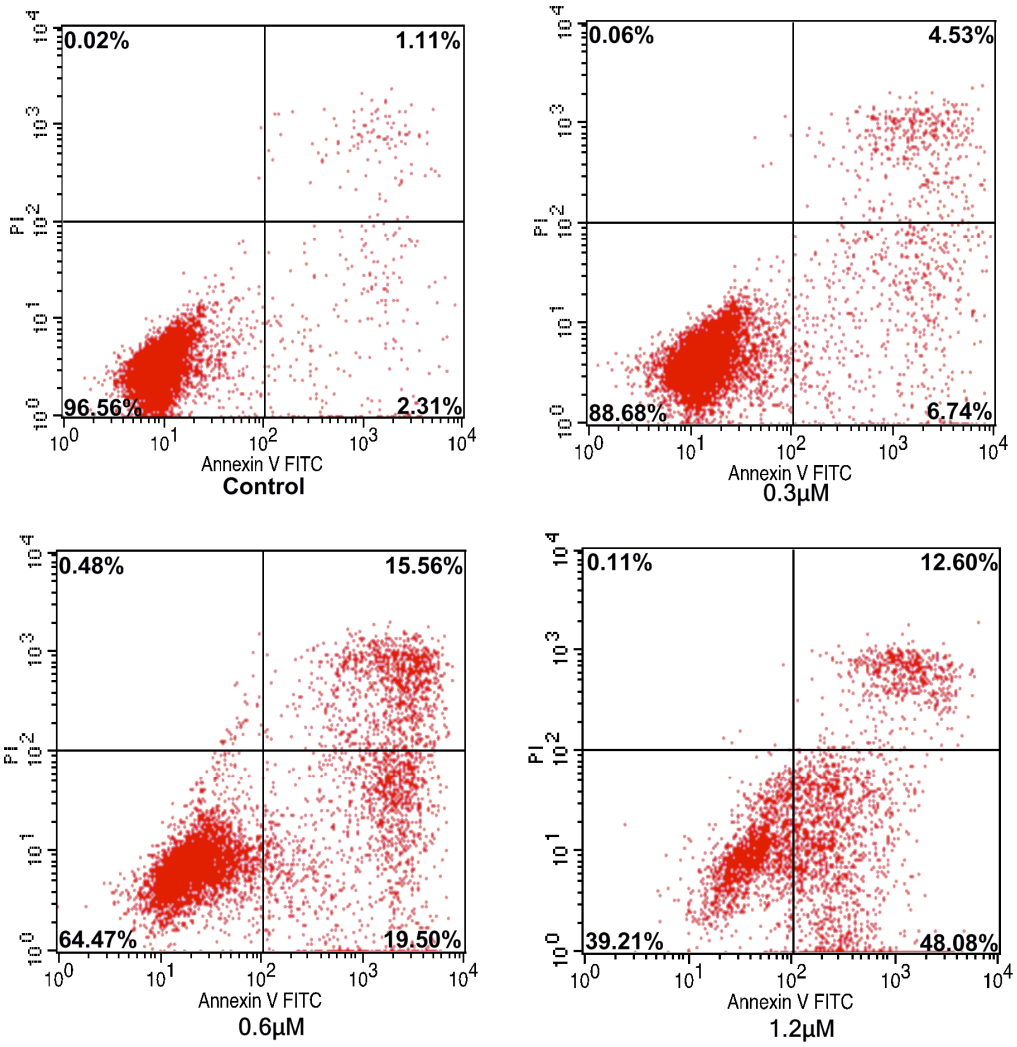

**Fig. 5**

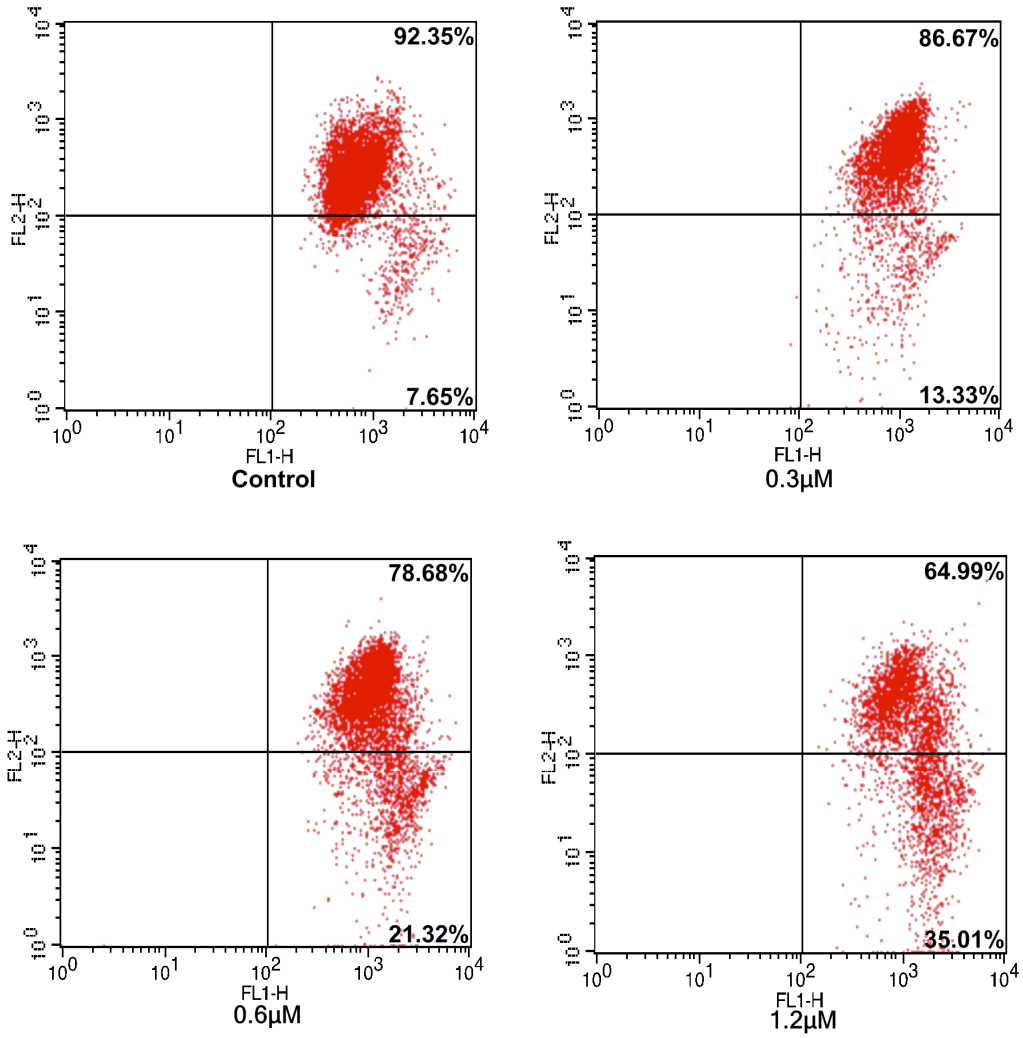

**Fig. 6**

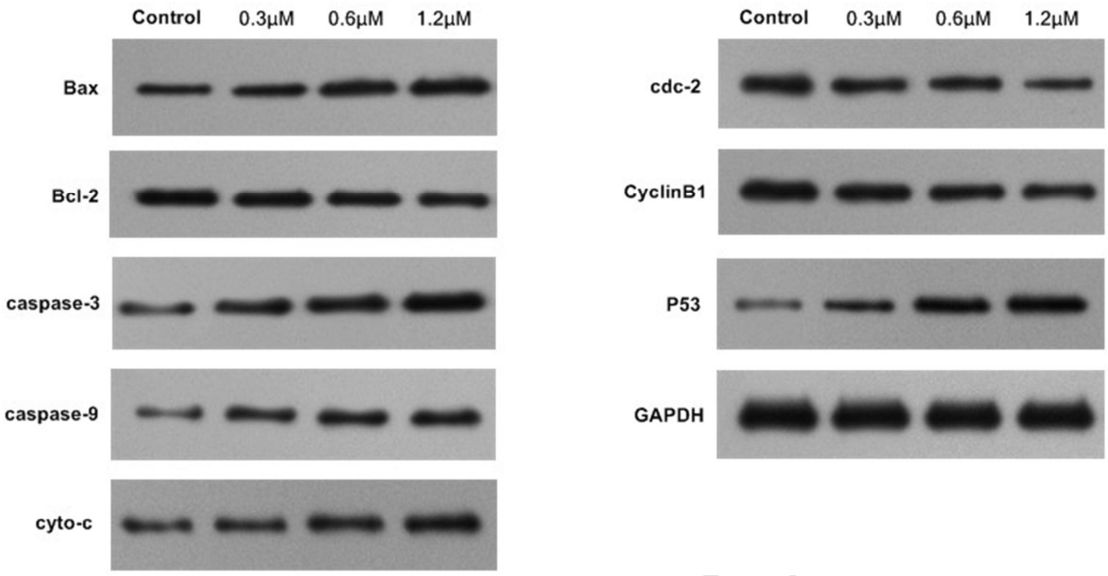

**Scheme 1**

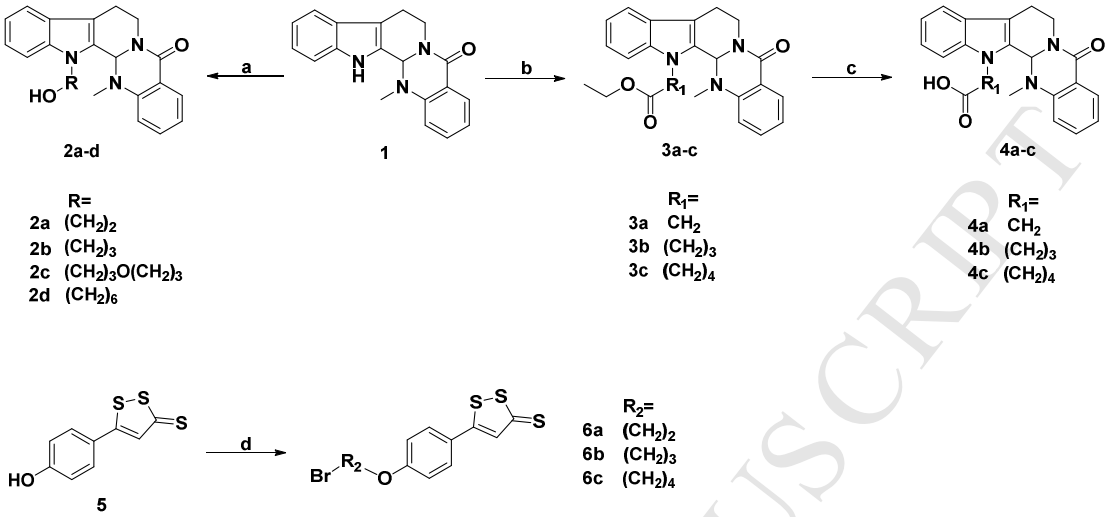

**Scheme 2**

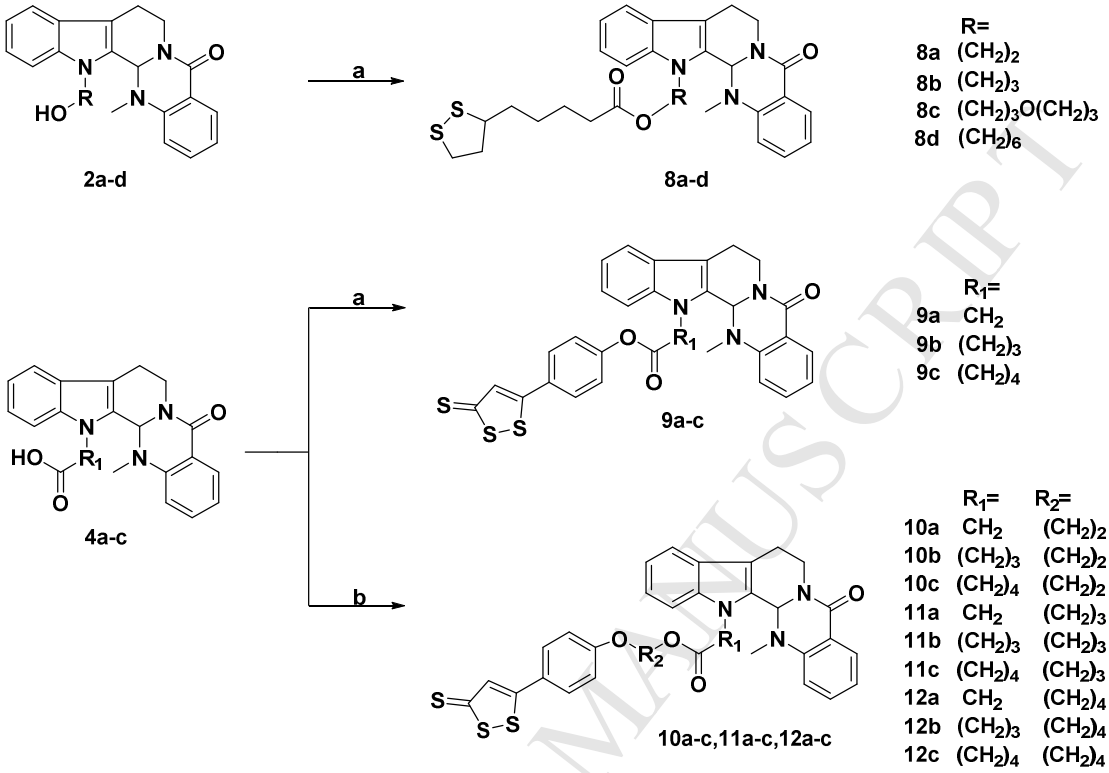

## Highlights

Two series of $H_2S$ donating evodiamine derivatives were synthesized.
**12c** showed good selectivity between human normal and tumor cells.
**12c** induced apoptosis and arrest cell cycle at $G_2$/M phase in HL-60 cells.
**12c** induced HL-60 cells apoptosis via the mitochondria-dependent pathway.